2019-01-01

Mesacs: A Multi-Method Environmental Study Over The Arctic Chukchi Sea

Julio Eduardo Ceniceros
University of Texas at El Paso, jeceniceros@hotmail.com

MESACS: A MULTI-METHOD ENVIRONMENTAL STUDY OVER THE ARCTIC CHUKCHI SEA

JULIO EDUARDO CENICEROS

Master's Program in Environmental Science

APPROVED:

Thomas E. Gill, Ph.D., Chair

Rosa M. Fitzgerald, Ph.D.

Miguel Velez-Reyes, Ph.D.

Jessie M. Creamean, Ph.D.

Charles Ambler, Ph.D.
Dean of the Graduate School

Dedication

I would like to dedicate this thesis to my family, friends and colleagues who always believed in me and provided the motivation and support for this research.

MESACS: A MULTI-METHOD ENVIRONMENTAL STUDY OVER THE ARCTIC CHUKCHI SEA

by

JULIO EDUARDO CENICEROS, B.A.

THESIS

Presented to the Faculty of the Graduate School of

The University of Texas at El Paso

in Partial Fulfillment

of the Requirements

for the Degree of

MASTER OF SCIENCE

Department of Geological Sciences

THE UNIVERSITY OF TEXAS AT EL PASO

May 2019

Acknowledgements

I would like to acknowledge the academic and professional support I received from my entire committee. Specifically, I would like to thank Dr. Jessie M. Creamean for providing me the opportunity to assist her Arctic research and for always being available to help me in my writing. I would also like to especially thank Dr. Thomas E. Gill who always provided me with great research opportunities and really pushed me to make the best out of this research experience. Thank you both for your continued professional advice and hope to keep these relationships going as I transfer into the professional research world. This thesis is based upon work supported by the National Oceanic and Atmospheric Administration, Educational Partnership Program, U.S. Department of Commerce, under Agreement No. #NA16SEC4810006. Thank you to NOAA's Center for Atmospheric Science and Meteorology (NCAS-M) for providing me with the fellowship that made this degree possible. The professional and personal development opportunities offered by NCAS-M really elevated my graduate student experience. To everyone involved, thank you for your time and support.

Abstract

The Arctic environment is a dynamic part of Earth's natural system and is currently undergoing rapid increasing air temperature and decreasing sea ice extent, leading to more open ocean waters. As open water areas become more prevalent, phytoplankton communities near the surface of the ocean can proliferate earlier in the year and are apt to reach higher concentrations by the end of the summer season. Phytoplankton biomass around the world has been known to produce a microscopic biofilm at the surface of the ocean composed of biogenic and biological particles which then become airborne and work as both cloud condensation nuclei and ice nucleating particles. These nuclei can subsequently impact the physical and radiative properties of clouds, thereby affecting the surface energy budget. Various studies have investigated the possible link between phytoplankton biomass and cloud condensation nuclei, but the distinct link between ice nucleating particles and the ocean has only rarely been explored, even more so in the high latitude Arctic environment.

A comprehensive multi-method study was executed to investigate marine aerosols originating from surface of the ocean and their role as ice nucleating particles in Arctic clouds over the Chukchi Sea. The overarching objective was to participate in a field study, in parallel with supporting lab and remote sensing techniques. The field study named Ice Nucleating over the ARCtic (INARCO II) provided excellent research experience for a graduate student to make local in situ measurements of both Arctic air and seawater. This study also explores for the first time how microscopic haloarchaeal species *Haloferax sulfurifontis, Natronomonas pharaonsis, Haloquadratum walsbyi,* and *Halococcus morrhuae* perform as ice nucleating particles. All four species have demonstrated some form of ice nucleating ability by nucleating ice at temperatures above homogeneous freezing $T \leq \sim -38℃$. The third study, remote sensing analysis, quantifiably characterized the Chukchi Sea phytoplankton biomass using satellite derived chlorophyll-a measurements as a tracer for phytoplankton biomass and its correlation to key cloud physical properties including ice cloud effective radius (re), ice water path (IWP), cloud-

top height (CTH), cloud-top temperature (CTT), cloud top pressure (CTP), phase, and cloud fraction at varying 1-km or 5-km spatial resolution. Correlation results and scatter plot linear fitting indicate a positive correlation between Chl-a concentrations with ice cloud effective radius (P-value = 0.0013 and R-value = 0.45) and cloud pressure (P = 0.0009, R = 0.46). Negative correlations were found between Chl-a with cirrus cloud reflectance (P = 0.0013, R = -0.45) and ice cloud optical thickness (P = 0.0267, R = -0.32). Spatial analysis results have shown that Chl-a concentrations do not increase evenly in exceptionally high months, but instead increase along the terrestrial coastlines with a weakening gradient leading to near zero concentrations in open ocean. Mean summer Chl-a concentrations for the entire Chukchi Sea showed a variable year to year summer season with a small increasing trend. Additionally, mean summer Chl-a concentrations were maintained between 1.4 mg/m^3 and 2.1 mg/m^3 in the past 15 years. Together this multi-method investigation produced results exemplifying the importance of considering Arctic plankton biomass and other biogenic INPs in future climatic models since changes in the sea surface concentrations appear to significantly influence certain Arctic cloud properties.

Table of Contents

List of Tables

List of Figures

1 Introduction and Motivation

The Arctic is spatially defined as the area north of the imaginary latitude line called the Arctic Circle (66° 33′N) as illustrated by Fig. 1.1 (Nyman, 2018). This remote part of the world hosts the Arctic Ocean, a year-round partially sea ice covered ocean alongside human populated land areas in Canada, Russia, Iceland, Norway, Greenland, and Alaska (Walsh, 2008). The Arctic Ocean is the smallest and shallowest of Earth's major oceans, making up around 3% of the Earth's surface and with an average depth of approximately 1,040 meters (Rudels et al., 1994; Serreze et al., 2000). The ocean's sea surface salinity (SSS) is distinct since it is sustained below 34 parts per thousand (ppt) compared to the world-wide ocean average at around 36 ppt (Boyer et al., 2005; Durack et al., 2012). The low SSS is thought to result from a combination of seasonal ice melt, high river run-off, and low rates of evaporation (Ardyna et al., 2017; Carton et al., 2015; Lammers et al., 2001). This high-latitude environment is home to unique human and wildlife populations that have evolved fascinating physiological adaptations like white fur on foxes or shorter thicker human bodies that radiate less heat compared to tropical human bodies (Gibson et al., 2015; Irvin, 2012; Laidre et al., 2015). Arctic wildlife includes arctic foxes, benthic epifauna and infauna, polar bears, seals, walruses, whales, and a large variety of avian and fish species (Chapin et al., 2015). Some of these species are endemic to the Arctic, and are now faced with anthropogenic induced climate variation resulting in unprecedented changes to their landscape, like the reduction of sea ice extent and thickness (Boeke and Taylor, 2018; Wang et al., 2018).

Arctic sea ice is by far one of the most important variables of the Arctic environment since it provides the structure on which diverse ecosystems are constructed on and is a major influence in controlling the overall Arctic surface radiation budget (Ramanathan et al., 1989;

Figure 1.1: Map by Nyman, 2018, depicting the Arctic environment situated north of the Arctic Circle at (66°33'N).

Wadhams, 2000). A surface radiation budget aims to understand and quantify how much sunlight reaches a general area, how it interacts with atmospheric and surface components found in that region and ultimately how much is absorbed as heat and how much is reflected back into space. Arctic sea ice works like a giant mirror reflecting a large portion of the sun's rays back into space, helping maintain the near surface summer average air temperature between 3 and 12℃ (Boeke and Taylor, 2018; Doney et al., 2012). During the Arctic summer season, solar radiation increases over the entire region and results in the reduction of sea ice cover, uncovering the darker open ocean below. Unlike frozen sea ice, exposed open ocean absorbs most of the sunlight and allows the surface water to heat up and subsequently contribute to future sea ice melt (Screen and Simmonds, 2010; Serreze and Barry, 2011). This reflective property (albedo) can be accurately quantified. The average albedo of bare sea ice is 0.5 – 0.7, while open ocean is at 0.06, meaning that bare sea ice usually reflects about 50% to 70% of sunlight and open ocean reflects only about 6% (Curry et al., 1996; Grenfell and Perovich, 1984). Hence, this natural process between the sea ice, the ocean, and the atmosphere can be characterized as a positive feedback loop for warming. In regard to environmental science, this feedback loop is recognized as Arctic amplification (Graversen and Wang, 2009; Pithan and Mauritsen, 2014).

Fig. 1.2 illustrates a simplified Arctic amplification loop created to illustrate the relationships between air temperature, sea ice cover, and open ocean. The positive or negative signs between the variables indicate either a negative or positive influence. Intertwined, a change in one variable directly affects the others. It is thought that Arctic amplification is the main cause for this region warming up twice as fast as the global average (Sun et al., 2016). Since the mid-20th century, average global temperatures have increased by 0.6 ℃ while the Arctic region has experienced an increase of 2 ℃ (Grebmeier, 2012; Johannessen et al., 2016).

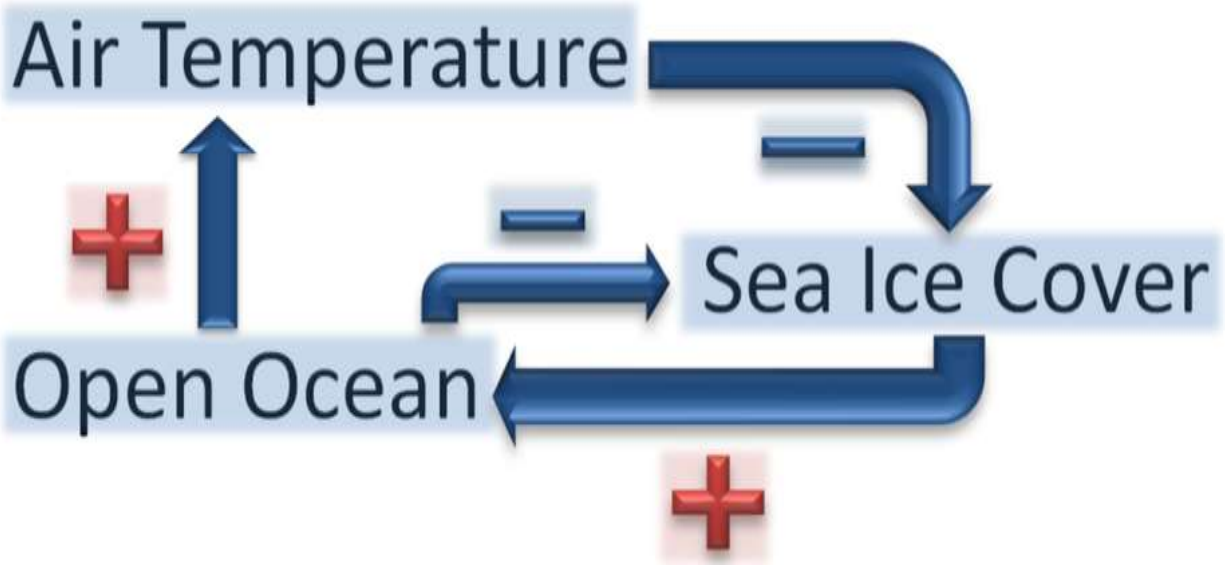

Figure 1.2: Simplified Arctic Amplification feed-back loop, the simplified diagram shows how natural variables found in the Arctic interact. Intertwined, a change in one directly affects the others.

The Arctic Report Card (www.arctic.noaa.gov/Report-Card/) produced annually by the National Oceanic and Atmospheric Administration (NOAA) considers a range of environmental measurements throughout the Arctic and has observed near surface air temperature continuing to increase at double the rate of the global temperature increase (Jeffries et al., 2015). Recently, anthropogenic influence in the form of increased greenhouse gases is starting to play a particularly important role in dictating air temperature and leading to historically low levels of ice cover (Najafi et al., 2015; Smith et al., 2017).

Yet, to truly understand and better represent the Arctic environment, this simplified model should also include key features such as clouds, marine plankton biomass, and aerosols. The reason for clouds is due to their strong influence in also controlling the Arctic's surface radiation budget. Clouds participate in two competing processes: warming the surface through the emission of longwave (LW) radiation and cooling the surface by shading the incident shortwave (SW) radiation (Shupe, 2016; Turner et al., 2018). Marine plankton biomass composed of phytoplankton, zooplankton, bacteria, viruses, and other trace microorganisms can be found in high concentrations near the surface of the ocean in the form of large ephemeral phytoplankton blooms or perennial hot spots along nutrient rich coast lines (Agawin et al., 2000; Tremblay et al., 2006). Plankton biomass requires sunlight in addition to nutrients to proliferate and thus was thought not able to develop until the sea ice started to retreat. However, light transmission through ice was enhanced by a recent increase in the fraction of first-year ice, which is much thinner (0.5 to 1.8 m) than the historically dominant multiyear ice pack (2 to 4 m), and especially by a high surface melt pond fraction (25 to 50%) (Arrigo et al., 2012; Post et al., 2013). Optical measurements showed that the ice beneath these melt ponds transmits fourfold more incident light (47 to 59%) than adjacent snow-free ice (13 to 18%) (Arrigo et al., 2012,

2014). Although the under-ice light field is less intense than open ocean waters, it was sufficient to support the blooms of under-ice phytoplankton, which grew twice as fast at low light as their open ocean counterparts (Kauko et al., 2019). Furthermore, it has been found that Arctic sea ice can be nutrient-rich if it has collected long-range transported dust sediment from surrounding terrestrial sources or captures phytoplankton in the ice as it froze (Cimoli et al., 2017; Meiners and Michel, 2017). Important minerals like iron can then fertilize the marine environment in the melting season and frozen algae can help sustain organisms like krill larva through the winter (Bluhm et al., 2017).

The importance in considering plankton biomass is due to their role in providing sources of marine bioaerosols (Simó, 2001; Wilson et al., 2015), specifically, marine exudate bioaerosols originating from microscopic particles at the surface of the ocean. Marine exudates and other organic and inorganic particles originate from biological ocean habitats below the surface, which then concentrate on the surface and finally ascend into the atmosphere through oceanic and atmospheric processes (Gershey, 1983). The world's oceans, not just the Arctic, are a major source of bioaerosols in addition to a myriad of microscopic particles in the form of sea spray (Brooks and Thornton, 2018; O'Dowd and De Leeuw, 2007). Organically enriched sea spray is mostly composed of sea salt (Na^+, K^+, $Mg2^+$, $Ca^{2+,}$ and Cl^-) and also includes bacteria, viruses, polysaccharides, proteins, lipids, and alkanes (Cochran et al., 2017; Reddy et al., 2018). Once airborne, these particles are then considered atmospheric aerosols and start interacting with radiation and atmospheric gases. In general, aerosols play a role in the surface radiation budget by scattering, reflecting, or absorption of the sunlight (Haywood, 2016; Nakata, 2018; Tomasi et al., 2017). The magnitude of the effect sea spray aerosols have on the surface radiation budget depends on the size, shape, and chemical composition of the individual particles (Nakata, 2018;

Suzuki et al., 2017). More importantly to this investigation are those aerosols with the ability to interact with clouds, given the required physical characteristics (DeMott et al., 2016; Quinn et al., 2017). These types of aerosols are classified as either cloud condensation nuclei (CCN) and/or ice nucleating particles (INPs). Further detail on CCN and INPs is presented later, but it is important to know now that both CCN and INPs can interact with clouds and alter their physical properties like albedo and cloud phase (Graf, 2004). Additionally, CCN and INPs can enable the formation of new clouds or can alter existing liquid, mixed-phased, or ice clouds (Fan et al., 2017; McCoy et al., 2015; Storelvmo, 2017). In essence, CCN facilitate the formation of water droplets by providing a surface for water vapor to condense over, while INPs facilitate the formation of cloud ice crystals by substituting the need to form a naturally formed ice embryo at low temperatures $T \leq \sim -38℃$ (i.e., pure water freezes at -38C) (Kanji et al., 2017; Kulmala, 2003). Finally, it has been identified that only a small amount of efficient INPs is needed to glaciate an entire cloud from mixed-phase to ice, resulting in changes in lifetime, precipitation, and albedo.

Fig. 1.3 illustrates a modified Arctic amplification feedback loop with the addition of plankton biomass, aerosols, and clouds. Although it is an improved depiction, this model is still lacking full representation of all variables involved in the actual Arctic environment. The real Arctic feedback loop involves dozens of more variables like animals and humans, but by understanding the dynamics between key variables like clouds and sea ice that remain uncertain, will provide modelers with improved process-level understanding for future generation Arctic models (Mysak and Venegas, 1998). Currently in the Arctic, a lack of parameterization for aerosol-cloud dynamics has resulted in large amounts of climate uncertainty in forecasting accurate future scenarios (Blanchard-Wrigglesworth et al., 2017; Semeniuk and Dastoor, 2018).

International aerosol and polar research meetings have both announced that source and implications of marine aerosols and their subsequent interaction with clouds remains greatly under parameterized and requires cross-scale research (Coluzza et al., 2017; Richter and Gill, 2018; Seinfeld et al., 2016).

Examining this simplified model, an ice-free summer season, with the influence of steadily increasing greenhouse gases, is a real possibility that would likely provide an increase in the plankton biomass' growing season. How would increases or decreases in plankton biomass alter INP concentrations in the lower atmosphere? Where are those sources of INPs located? Have plankton biomass concentrations changed in the past few decades, and if so, in what ways? Are ice cloud properties changing when plankton blooms are underneath? How do the individual constituents of sea spray influence the total effect it has on the environment? All of these questions justified the creation of a multi-method thesis investigation that involved precise field research, in parallel with supporting lab and remote sensing analysis. This top-down and down-up perspective combines local in-situ measurements with regional satellite perspectives to produce cross-scale results and implications. Compared to only a single methodology, by approaching the same scientific question using a variety of methods has led to a more natural multidisciplinary understanding.

The aforementioned observational gaps highlighted in Fig. 1.3 have motivated the direction of this thesis with the overarching objective of improving physical process-level understanding between the Arctic plankton biomass, aerosols, and ice clouds for the enhancement of modeling capabilities. The three main research components involved in this investigation are the following:

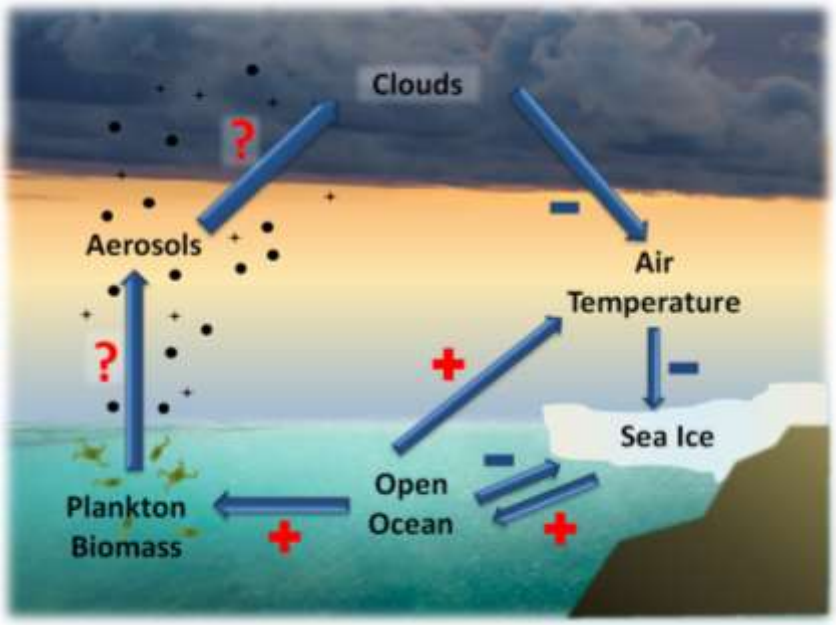

Figure 1.3: Modified Arctic amplification loop, this diagram represents a more complete system that includes plankton biomass, aerosols, and clouds. The way these variables interact is still lacking parameterization for accurate model representation.

1) Participating in a field setting as a student assistant on a summer 2018 NOAA/Colorado State University Arctic shipborne field campaign called Ice Nucleation Over the ARCtic Ocean II (INARCO II).
2) Testing the efficacy of marine dwelling archaea microorganisms as potential INPs in a lab setting.
3) Creating a satellite-based climatology of plankton biomass and correlation between plankton concentrations with physical and optical cloud measurements aloft in the Chukchi Sea.

This investigation has concentrated on both the regional- and local-scale with the desire to produce cross-scale results. Each of the three research components will include their own objectives, methodology, and results, which will then be combined to enhance Arctic aerosol-cloud processes, marine INP sources, and a look back into the interconnected history of Arctic plankton and ice clouds. Since field research in the Arctic is expensive and requires high amount of logistical planning, the area of focus and to represent an Arctic environment is the Chukchi Sea.

2 Regions of Interest and Background

2.1 Chukchi Sea

The Chukchi Sea is located off the north and west coasts of Alaska and situated directly above the Bering Strait. This area was chosen to represent the Arctic environment for several reasons. It includes important fishing grounds for the United States and can sustain strong and long-lasting summer average concentrations of surface chlorophyll-a around 21.7mg m^3 (SD = ±19.6 mg m^3) and 54.5 mg m^3 (SD = ±67.7 mg m^3) for the northern and southern regions, respectively (Courtney et al., 2016; Yun et al., 2016). The sea has a surface area of approximately 595,000 km^2 (230,000 sq. mi) and although expansive, it is mostly underlined by the underwater Chukchi Plateau raising the average depth to only ~50 m (Overland and Roach, 1987; The Atlas of Oceans, 1980). Seasonally frozen over, sea ice starts to freeze in October in the north which then extends southerly until the entire sea is typically frozen over by December (Serreze et al., 2016). The sea remains frozen until approximately late April at which point the sea thaws in the opposite direction from south to north (Stroeve et al., 2016).

High nutrient availability patterns in the sea water play an important role in dictating where phytoplankton can develop providing a steady source of food for plankton in the Bering Strait and the Chukchi Sea to fuel primary production. In addition to sunlight, water, and carbon dioxide, phytoplankton require nitrogen, phosphorous and iron. Iron in marine ecology and oceanography is now of substantial attention due to its ability to limit primary production. Because iron is essential for metabolism and nitrogen usage, chlorophyll biosynthesis and other cellular respiratory systems in phytoplankton are limited by iron availability and therefore play an important role in the ocean net primary productivity. The hydrology of the summer Chukchi waters includes three distinct bodies of water typically flowing north through Bering Strait

(Weingartner et al., 2005). Nutrient rich Anadyr Water (AW) tends to flow through the most westerly side of the strait, while less nutrient Alaskan Coastal Water (ACW) flows through the eastern extent of the strait (Danielson et al., 2017; Nishino et al., 2016; Stein et al., 2017). Between those two bodies of water, relatively low nutrient Bering Shelf Water (BSW) squeezes through. This narrow passage forces AW and BSW to mix and produce new combined Bering Shelf Anadyr Water (BSAW) that tends to flow northerly but has been observed to reverse direction due to wind shear forcing during summer storms (Iken et al., 2018; Stabeno et al., 2018). Alaskan coastal water remains mostly unmixed and flows north along the Alaskan coast as its name implies (Gong and Pickart, 2015).

2.2 Marine Boundary Layer Aerosols

The term aerosol in its most basic definition is any solid or liquid particle suspended in a gas (Wallace and Hobbs, 2006). In regard to the study of environments, the scientific term aerosol is usually in reference to Earth's atmospheric aerosols. The types of aerosols found in Earth's atmosphere are both natural and anthropogenic in origin and range from single nanometers to a few centimeters in size (Hartmann, 2015; Wallace and Hobbs, 2006). The composition of aerosols varies globally, and sources can have a steady input of particles like sea spray, while others are marked by intense but short-lived events like volcanic ash eruptions (Calvo et al., 2013, Kanji et al., 2017). The volume of a liquid droplet or the size of a particle is a major factor in determining the atmospheric residence time for the individual drops or particles (Kunkel, 1984; Wallace and Hobbs, 2006). This research focuses on Arctic marine boundary layer aerosols especially those that are capable of interacting with clouds and originating from the marine environment.

The Arctic atmosphere is a dynamic natural system noted by low temperatures, half a year of reduced solar radiation, low water vapor amounts, and frequent temperature inversions (Palo et al., 2017; Walsh et al., 2018) The Chukchi Sea seasons are further discerned by pronounced fluxes of anthropogenic pollution (Kanji et al., 2017; Vinogradova, 2015). The winter and spring seasons are characterized with peak infiltration levels of pollution originating largely from Eurasia (Monks et al., 2015; Wallace and Hobbs, 2006). The summer season has relatively "cleaner" marine boundary layer air and is recognized as the pollution minimum season. Summer samples of aerosols in the Chukchi Sea marine boundary layer have shown the composition of aerosols to be a mix of ship emissions (containing S, Fe, V, and Ni), anthropogenic pollution (containing Cu, Zn, Pb, and Hg), crustal elements (containing C and Fe), and sea spray (Curry, 1995; Xie et al., 2006). The dominant component in sea spray is sea salt (NaCl) but also includes organic material associated with phytoplankton cell exudates concentrated on the surface microlayer (Wallace and Hobbs, 2006; Wilson et al., 2015). The marine biogenic particles at the surface microlayer become airborne through the physical process of bubble bursting (Resch et al., 1986; Wilson et al., 2015). Bubbles from the subsurface and cresting waves both spray particles into the air. Bubble dynamics can be quite detailed with studies showing a correlation between bubble size and the size range of sprayed aerosols (Ault et al., 2013; Veron, 2015). These and other biogenic particles are lab-proven INPs and can be produced in vast quantities during the summer season (Kanji et al., 2017; Wilson et al., 2015). Characteristics of Arctic marine INPs include that they are biogenic in origin, <0.2 micrometers, and nucleate ice at temperatures relevant to mixed-phased and high-altitude cirrus clouds (DeMott et al., 2010; Xie et al., 2006). Phytoplankton with their green chlorophyll pigment feed the plankton and subsequently help in the production of exudate particles; albeit identifying the

full spectrum of biogenic material of Arctic water and their emission locations remains an area of strong international investigation (Creamean et al., 2018b; Quinn et al., 2007). Bacteria are a robust component in terrestrial biogenic INPs so it is justified to believe that marine bacteria should also be an important source of marine biogenic INPs (Kanji et al., 2017).

2.3 Ice Nucleation

Natural formation of ice in the atmosphere occurs mostly in correlation to temperature (DeMott et al., 2010). If the relative humidity is high enough in the atmosphere, water vapor can change phases directly into an ice crystal through sublimation. Ice can also be produced by lowering the temperature of a preexisting water droplet below a temperature threshold to freeze the drop through the process known as homogeneous freezing at around $T \geq \sim -\mathbf{38}$℃ (Fletcher, 1959; Herbert et al., 2015; Zhao et al., 2018). If no foreign particles reside inside the droplet then homogenous threshold temperature is correlated to the volume of the drop (Wallace and Hobbs, 2006). A supercooled liquid drop is energetically unstable and can achieve freezing in a variety of mechanisms in addition to homogeneous freezing. Special particles with the right prerequisites are called INPs (DeMott et al., 2010). INPs interact with water droplets and facilitate warmer freezing temperature thresholds through heterogeneous freezing mechanisms (Wallace and Hobbs, 2006). There are four types of heterogeneous freezing modes and all include the presence of a suitable particle that interacts with the water droplet in one way or another. *Deposition nucleation* is the circumstance in which relative humidity is high enough for water vapor to phase change directly into ice using the INP as an ice embryo (Kanji et al., 2017). *Immersion freezing* is when a particle is inside the droplet and can provide a stable surface for the water molecules to organize and overcome the need for a natural ice embryo (Cziczo et al., 2017; Kanji et al., 2017). *Contact freezing* is the situation when a particle in the air comes in

contact with a supercooled droplet and induces very quick freezing usually at warmer temperatures compared to immersion freezing with the same particle (Collier and Brooks, 2016; Hande et al., 2017; Wallace and Hobbs, 2006). Lastly, *condensation freezing* includes a CCN to form a water droplet followed by the immediate freezing due to either contact freezing or immersive freezing, which can be induced by the insoluble portion of the CCN (Kanji et al., 2017; Wallace and Hobbs, 2006). The volume of a drop is also relevant in heterogeneous freezing since increasing the drop volume simultaneously increases the probability of hosting an efficient INP (Wallace and Hobbs, 2006). The temperature at which certain INPs can facilitate freezing in the atmosphere depends, in general, on the concentration of INPs found in the troposphere, the chemical composition, shape, size, and preactivation history (Wallace and Hobbs, 2006). Under high altitude cirrus cloud temperature ($T \leq -20℃$) deposition freezing was observed to be the most common mode of freezing (Cziczo et al., 2017).

In order for a particle to have ice nucleating abilities, it must possess certain types of nucleus particle prerequisites. For insoluble particles that can remain solid in a water droplet, they must possess microscopic highly receptive ice activating sites on their surface area. Activation sites can be designated either as structural lattice or hydrogen bond based. Structural lattice activation sites include a lattice match between the ordered hexagonal bilayers of the particle crystal lattice with the hexagonal crystal habit of ice (Kanji et al., 2017; Wallace and Hobbs, 2006) The similarity between molecular structures facilitate the organization of the water molecules playing the role of an ice embryo (Murphy, 2003). Empirical studies have shown that silver iodide and certain volcanic ash particles mainly nucleate ice through this structural lattice match (Kanji and Abbatt, 2006; Welti et al., 2009). Hydrogen bond activation sites include areas that actuate hydrogen bonds with water molecules based on available oxygen at the edges of

certain particles, such the case with functional hydroxyl group particles (Freedman, 2015; Sihvonen et al., 2014). In general, the ice nucleation ability of a solid particle will be contingent on the lattice structure shape, size, surface area, and chemical composition (Welti et al., 2009). Soluble particles, such as organic protein complexes found on cell membranes, facilitate the formation of ice again using hydrogen bonds (Pummer et al., 2015; Wallace and Hobbs, 2006). Other biological fragments also include pollen, fungal spores, marine organic aerosol, and organic material found in soil (Kanji et al., 2017; Xie et al., 2006; DeMott et al., 2010). Biological fragments are known to attach to other larger particles and play an important role in dictating the larger particle's ice nucleating abilities (DeMott et al., 2016; Hartmann et al., 2013).

Global yearly emissions of dust from deserts, volcanoes, and soil have been calculated between 1950 to 2400 Tg yr^{-1} (Ginoux et al., 2001; Ginoux et al., 2004). Mineral and desert dusts are relevant atmospheric aerosols due to their high abundance and capable ice nucleation abilities well above homogeneous freezing (Barahona et al., 2017; Huang et al., 2018). The mineral group K-feldspar (possibly microcline, one of the two K-feldspar end members) has been identified as the most ice-active component in dust with the exposed lattice plane promoting ice nucleation. The amount of K-feldspar, size, and particle concentrations are all key aspects that dictate dust's overall ice nucleating effectiveness (Kanji and Abbatt, 2006; Welti et al., 2009).

Bioaerosols are those biological particles that are from organic origin and become airborne (Kanji et al., 2017; Prenni et al., 2012, Wilson et al., 2015). They differ from biological fragments in that they are usually larger in size and can be a mix of soluble and insoluble components (Alpert et al., 2011; Huffman et al., 2013). Bioaerosols include bacteria, fungal spores, pollen, viruses, phytoplankton, lichens, and marine exudates, all of which have ice nucleating abilities at T < -15℃ with bacteria capable of nucleating ice at warm temperatures

around ~-1℃ (Augustin et al., 2013; Pummer et al., 2012; Wex et al., 2015). The ice nucleating ability of bioaerosols will depend on the type and also the tropospheric concentration (Kanji et al., 2017). Sources of bioaerosols include the world's oceans, vegetation, soils, lakes, and living organisms. The oceans are of key interest to this investigation and are known to emit bacteria, archaea, protozoa, and phytoplankton (Hiranuma et al 2014; Mason et al 2015). The global marine emissions of submicron primary organic aerosol particles by sea spray have been estimated to be 10 ± 5 Tg a^{-1}.(Facchini et al., 2008; Kanji et al., 2017) A gap in understanding and quantifying total concentrations, fluxes, and ice-nucleating properties of all types of bioaerosols in the marine atmosphere remains as an area of strong global research interest.

One of the most common bioaerosol INPs found in nature are bacteria, found abundantly all over the world (Kanji et al., 2017; Wex et al., 2015). Soil dust is another large source of aerosol since a large portion of Earth's land cover is dedicated to agriculture and farming (O'Sullivan et al., 2018). Soil dust is an efficient INP similar to desert dust with the key difference of soil dust having heavy internal mixing with organic material (Hill et al., 2016; Tobo et al., 2013). This has been proven by heat treating soil dust up to 90 - 100℃, resulting in the reduction of ice nucleating capability of the dust particles (O'Sullivan et al., 2014; Tobo et al., 2013). Freshly milled soil dust has been known to nucleate ice at warmer temperature compared to older soil dust (DeMott et al., 2016; Kanji et al., 2017). This is thought to be a result of the fresh soil dust retaining organic fragments before they fall off during air transport as time passes (Fröhlich-Nowoisky et al., 2014).

Biomass and fossil fuel combustion aerosols are similar in the sense they are both produced in the burning of organic material but differ in chemical composition. Fly ash and smoke are both a result of biomass burning of forests, agricultural fields, and wood in stoves

capable of short- and long-range transport (Gibbs et al., 2015; Kanji et al., 2017). Fossil fuel burning is different by the fact that it additionally produces large amounts of soot, also known as black carbon (Kanji and Abbatt, 2006). Black carbon can still nucleate ice but is mostly recognized to freeze at lower temperatures close to that of homogeneous freezing around T< ~-40℃ (Abbatt et al., 2006) Volcanoes are a prolific source of aerosol with an estimated ~13 Tg yr^{-1} in global yearly emissions (Dentener et al., 2006). Volcanic ash is capable of ice nucleating via deposition at around -13 to -23℃, but is also known to nucleate ice up to -8℃ via contact freezing (Gibbs et al., 2015). The chemical composition and thus ice nucleating capability of volcanic ash will vary per volcano with certain types of ash not capable of inducing freezing via contact freezing (Gibbs et al., 2015; Zolles et al., 2015). Similar to other atmospheric aerosols, volcanic ash will display unique ice nucleating characteristics based on tropospheric concentrations and composition (Kanji et al., 2017, Wallace and Hobbs, 2006). Finally, one of the most common marine aerosols is crystalline salt (Cziiczo et al., 2013). Salt aerosols are emitted mostly from the world's oceans and some smaller sources are also found on land, such as arid dried lake beds called playas (Reynolds et al., 2007). Over the ocean, around 25% of all cirrus cloud ice residue samples included a type of salt (NaCl, NaI, Kl, KCl) (Abbatt et al., 2006, Fröhlich-Nowoisky et al., 2014; Kanji et al., 2017). Salt crystals for the most part will be >25 μm in size and are thought to induce freezing mostly through heterogeneous contact freezing (Wagner et al., 2016). Salt crystals are also efficient CCN so immersive freezing might also come into play if the salt crystal has interacted with some organics or other atmospheric components as it ascended into the high cirrus elevation (Fröhlich-Nowoisky et al., 2014).

Preactivation of INPs is when a porous particle undergoes freezing at a certain temperature followed by the thawing of the ice crystal but leaving ice still intact inside the pores

(Wagner et al., 2016; Wallace and Hobbs, 2006). This process then results in the same particle now having a different freezing temperature, usually $\pm 5℃$ from the original (Wallace and Hobbs, 2006). It is thought that this is due to liquid or still frozen water inside pores and cracks in the particle (Cziczo et al., 2013; DeMott et al., 2010). If ice is present anywhere on the particle then it will serve as a highly effective ice activation site (Vali and Stansbury, 1966). The preactivation efficiency is linked to pore size peaking at a pore size range of 8 – 10 nm for best increased ice nucleating efficiency (Wagner et al., 2016). A source of atmospheric ephemeral freezing for a particle has been observed inside air parcels that pass over an airplane wing (Vali al., 2015). The quick contraction and expansion of the air will sometime momentarily produce an ice crystal, which will then just as quickly almost entirely thaw, leaving behind a preactivated INP (Kärcher et al., 2009). A lot of information still remains unknown in the process of preactivation leading to a source of ambiguity regarding INP field sampling since the history of the particle is usually not known.

In the Arctic there are several large sources of INPs at play, including both terrestrial and marine sources and also both short- and long-range transported INPs (Baddock et al., 2017; Pithan and Mauritsen, 2014). During the summer season in the Chukchi Sea we expect low levels of anthropogenic pollution but understanding if increased phytoplankton distributions play a role in sources of marine INP locations still remains unknown. A growing community of Arctic research is focusing on long-range dust sources whose emissions and impacts additionally remain uncertain (Abbatt et al., 2019; Coopman et al., 2018; Tobo et al., 2019). Marine INP sources in the Arctic are hypothesized to play a more significant role in the summer season since less anthropogenic pollution will be present (Kanji et al., 2017).

2.4 Archaea

The domain Archaea was only recently officially recognized after being proposed by Woese et al. (1990) as the third branch of life by using their 16S rRNA genetic technique. The revolutionary genetic technique developed in 1971 takes use of 16S rRNA sequences as molecular clocks for prokaryotes (Woese and Fox, 1977). Due to morphological similarities, pre-1990 archaea were incorrectly classified under the domain Bacterium as genus *Archaebacteria*. Since then, extensive research using the complete archaea genomes available through the National Center for Biotechnology Information has allowed archaea to taxonomically branch out into a formidable prokaryote domain consisting of 63 genera and 209 species.

Archaea are sometimes referred to as "extremophiles" since they have conserved remarkable morphological adaptations that allow them to live and proliferate in extreme environments such as hypersaline lakes (NaCl concentrations >10%), acid mine drainage (pH near 0), and temperatures ranging from below the freezing point to above the boiling point of water (Rothschild and Mancinelli, 2001; Baker-Austin and Dopson, 2007). Since these conditions are normally uninhabitable by most other organisms, archaea are known to dominate these sometimes spatially expansive environments. The taxonomic class haloarchaea in particular, is found in solutions with ≥ 5% salt weight to volume (w/v) and can dominate natural hypersaline habitats. For example, the Great Salt Lake in Utah can sustain densities of 107–108 archaeal cells ml^{-1} or higher (Oren, 2002; Deming and Collins, 2017; Lindsay et al., 2017).

However, members of this diverse domain are also found outside extreme environments in aerobic marine and soil environments such as sea water, agricultural soil, and even on human skin (Schleper, 2005; Wehking et al., 2018). It is now estimated that archaea represent ~10% of

prokaryotes found in the earth's biosphere (Fröhlich-Nowoisky et al., 2014). In regard to the world's shallow and deep oceans, archaea cell numbers are estimated around 1×10^{28} archaeal cells compared to 3×10^{28} bacterial cells (Karner et al., 2001; Massana et al., 1997).

The presence of these natural microorganisms is relevant to this investigation because similar to bacteria INP sources, archaea are known to become airborne and reside in the atmosphere as bioaerosols (Choudoir et al., 2018). Bacteria and archaea have been collected in aerosol samples and typically appear in mixed particle clusters ranging in size from ~2 μm to ~4 μm, which can travel short or continental distances (Després et al., 2012). There is a large amount of literature providing evidence that both intact bacterial or bacteria cell fragments are efficient INPs able of nucleating ice up to -1℃ (O'Sullivan et al., 2018; Welti et al., 2009). Furthermore, intact and fragmented cell parts of known marine dwelling bacteria and archaea have been collected in coastal aerosol samples providing evidence of natural ocean-atmosphere forces driving microscopic particles out of the sea surface and into the troposphere. Several prokaryote INP studies have concentrated on bacteria, although no investigation has ever previously tested the INP efficacy of any archaea species in a controlled lab setting.

2.5 Remote Sensing

High latitude studies involve unique challenges due to traveling to remote locations, harsh weather conditions, and expensive equipment, thus, satellites provide an advantageous top-down perspective capable of much larger spatial and temporal coverage over the Arctic. Satellites allow the observations of both atmospheric and marine environments allowing this investigation to take use of image data of both clouds and plankton biomass. A major component of plankton biomass is phytoplankton, aquatic microscopic algae that contain chlorophyll similar to terrestrial plants. Chlorophyll is what gives both marine and land

Figure 2.1: Diagram from Blunden and Arndt, 2016 listing the long-term changes observed in the Arctic. Record sea ice retreats and increasing marine primary productivity all indicate a changing environment.

vegetation their distinctive green color, and it is this green pigment that satellites are able to detect from space. Satellite measurements refer to this pigment as chlorophyll (Chl-a) expressed in concentrations (mg m^{-3}) and can be used as a proxy for marine plankton biomass concentrations. Although satellite observations do provide a useful regional perspective, they are restricted to only very superficial sea surface concentrations and cannot penetrate down into the water column.

Long-term remote sensing climatological studies of the Arctic have indicated that the Arctic Ocean exhibited a statistically significant 20% increase in marine primary productivity between the years of 1998 - 2009 due to secular increases in both the extent of open water (+27%) and the duration of the open water season (+45 days) (Fig. 2.1) (Laidre et al, 2015; Blunden and Arndt, 2016). Overall, various and diverse signals indicate the Arctic environmental system continues to be influenced by long-term increasing trends in air temperature (Hill and Cota, 2005).

Since Charlson et al. (1987) suggested that marine algae participate in climate regulation through the production of the cloud precursor dimethylsulfide (the CLAW hypothesis, so called after the authors' initials), much experimental effort has been invested in exploring the links between oceanic plankton infused sea spray and marine clouds (Lana et al., 2012). The role of ocean biota in modifying chemical composition and size distribution of both CCN and INPs has been observed and proven a potentially key component in modulating pristine ocean cloud microphysics (Meskhidze and Nenes, 2007). In the Arctic, recent studies have shown that biological INPs can originate from the ocean and can be associated with areas of high biological activity (DeMott et al., 2010; Xie et al., 2006; Wilson et al., 2015). This recent awareness has motivated this particular remote sensing research segment and is dedicated to exploring the link

between concentrations of surface plankton biomass and optical and physical cloud properties over the Arctic Chukchi Sea.

Clouds have consistently been difficult to model since the processes dictating their occurrence, lifetime, and microphysics are heterogeneous in nature and vary across scales. Aerosols are a main component of cloud development and will manifest distinct cloud formations based on their size, composition, and number distributions. Key measurable cloud variables represented in current models include cloud effective radius, ice/liquid water path, cloud-top temperature, cloud top pressure, cloud emissivity, cloud optical thickness and cloud fraction. Understanding the multi-scale processes controlling these variables will undoubtedly help better represent clouds in atmospheric models.

3 Methods

3.1 Ice Nucleation Over the Arctic Ocean I and II (INARCO I/II) Field Campaigns

The understanding and observational studies of marine sources of INPs in the Arctic remain extremely limited. The majority of research and measurements in regard to in situ marine plankton biomass and lower atmosphere INP concentrations are mostly reported at mid-latitudes or the Southern Ocean (Kanji et al., 2017). Specifically, the natural processes regarding Arctic clouds and their interactions with aerosols are ineffectively understood and remain a source of ambiguity for Arctic modeling capabilities (Blanchard-Wrigglesworth et al., 2017; Semeniuk and Dastoor, 2018). Additionally, understanding which constituents of marine plankton biomass are responsible for the warmest glaciation temperatures still remains a challenge (Barthel et al., 2019; Hallegraeff , 2016; Quinn et al., 2017). INP sources and their atmospheric presence in the Chukchi Sea vary greatly with location and can have very different freezing points, such as -5 ℃ from marine microsurface samples or -13 ℃ from aerosol samples over Bering Strait (Creamean et al., 2018b; DeMott et al., 2016).

The combination of the Arctic summer having increased cloud cover, precipitation, and plankton biomass make it the perfect time for shipborne field research regarding aerosol-cloud interactions. The cooperative effort between Distributed Biological Observatory – Northern Chukchi Integrated Study (DBO-NCIS) and INARCO I/II provided the necessary infrastructure and organization to make this type of investigation possible. The three-week 2017 and 2018 summer ship expeditions on board *Healy* allowed sampling of various Chukchi Sea water columns and aerosol sampling for INP concentration analysis. The main hypothesis tested during field research was the notion that Arctic marine INP sources are constantly dependent on ecological, oceanographic, and atmospheric processes.

3.1.1 INARCO I

Prior to the INARCO II field campaign that took place in August, 2018, I spent the early summer of that year participating in an internship with NOAA's Earth System Research Laboratory (ESRL) in Boulder, CO. Under the supervision of NOAA researcher at the time - and now Colorado State University researcher - Dr. Jessie M. Creamean, I spent two months at the lab investigating microbial particulate material from Arctic air and sea water samples. These samples were collected in summer 2017 during INARCO I. Using a lab-based immersive freezing technique I tested how the microbial particulate material might affect the formation of ice crystals in Arctic clouds by serving as INPs. These analyses helped finish the remaining samples of INARCO I, documenting and understanding ongoing changes to the Pacific-Arctic ecosystem in light of the changing physical drivers. INARCO I took place August 26, 2017 – 13 September 13, 2017 and included the sampling of designated DBO- NCIS transects 1 – 5 (Fig. 3.1).

DBO-NCIS is a multidisciplinary Arctic Ocean sampling program supported by the NOAA's Arctic Research Program (Grebmeier et al., 2012). Furthermore, it designated eight "hot spots" areas across the Bering, Chukchi, and Beaufort Seas where multidisciplinary sampling is focused (Fig. 3.1b). These "hot spots" have been chosen because of their high concentrations of ecosystem productivity, biodiversity, and overall rates of change. Methodology of both sea water and aerosol sampling is explained in the following subsections.

3.1.2 INARCO II

On August 7, 2018 my research teammates and I traveled to Nome, AK where we began our 3-week INARCO II shipborne field campaign through the Bering and Chukchi Sea. Our research team consisted of 4 students led by principal investigator (PI) Dr. Jessie M. Creamean.

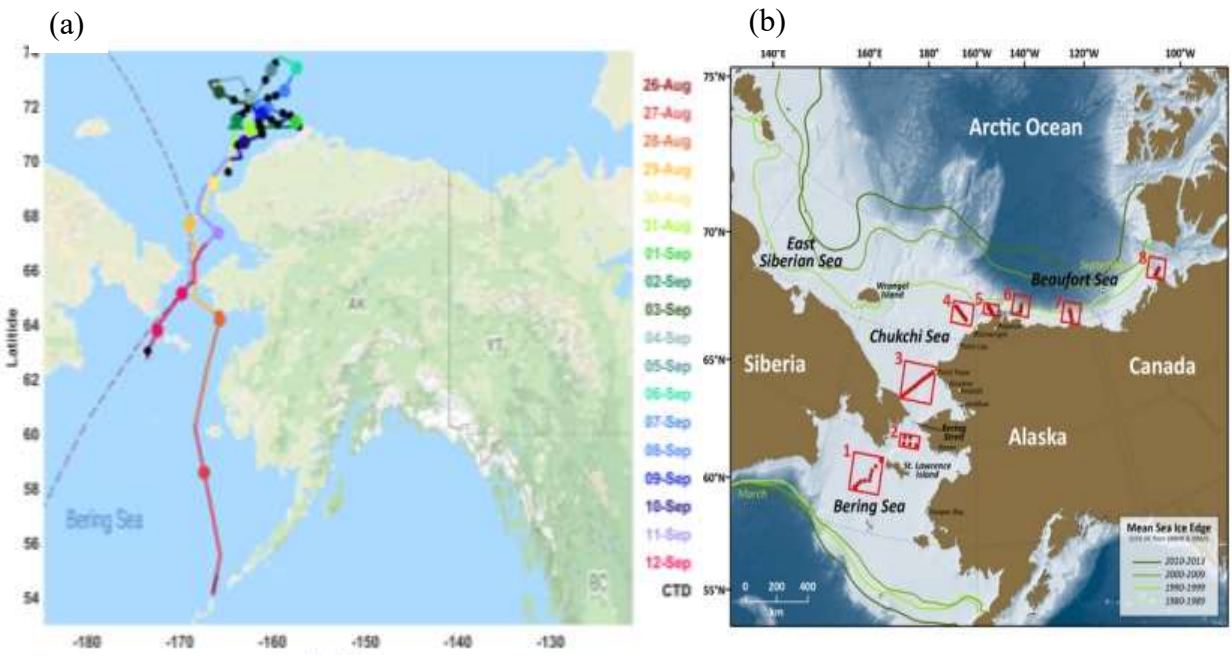

Figure 3.1: (a) Map created by Creamean et al. (submitted) illustrating the ship route during INARCO I. (b) Map from NOAA Arctic website (www.arctic.noaa.gov) pointing out the 8 transects measured yearly as part of the NOAA's DBO-NCIS program.

Taylor Aydell, a graduate student from San Jose State University and undergraduate Nadia Colombi from University of California, Los Angeles were supported through the NOAA Ernest F. Hollings Scholarship program. Graduate student from the University of Miami, Emily Bolger, was funded by NOAA's Arctic Research Program and I was funded by the NOAA Experiential Research & Training Opportunities (NERTO) program. We started by arriving in the port town of Nome, AK, which was were where we would board the 7-deck, 420-foot-long *Healy* and meet the other 42 participating scientists. The 43-member international and multidisciplinary team of scientists on board *Healy* consisted of 5 scientific groups made up of oceanographers, biologists, ecologists and atmospheric scientists. My team's investigation objective included understanding ocean-atmosphere boundary processes. Working 12-hour shifts our team rotated to keep a 24-hour scientific consecration on collecting samples, running analyses, and data organization.

3.1.3 Collection Methodology

Sea water samples were collected starting August 7, 2018 until August 24, 2018 using *Healy's* under way system inlet 8 m below the surface and collected at 1600 UTC every day. Various conductivity, temperature, density rosettes (CTDs) were deployed along DBO transects to collect sea water samples almost every day. CTDs rosettes are a very valuable piece of field equipment used in oceanography. The rosette refers the metal framework that hold 24 10-L Niskin™ bottles for collection of sea water samples. CTD and other sensors are located at the bottom of the frame and will measure multiple water variables such as oxygen concentration as it descends. Preparation includes opening the top and bottom of all 24 bottles and calibration of sensors. The CTD then steadily descends to the bottom of the ocean and real-time measurements from the sensors are displayed on a computer monitor as water column profiles. Through the computer we also signal individual bottles to close at different depths to collect different types of

waters. All sea water samples were analysed on board for INP concentration immediately after collection. Sea ice was also collected on a single occasion, which then proceeded to be sealed, melted at room temperature, and analyzed onboard like the other sea water samples. CTDs allowed us to observe INP activity throughout the entire water column.

Aerosol samples were collected using a 4-stage time- and size-resolved Davis Rotating-drum Universal-size-cut Monitoring (DRUM) single-jet impactor (DA400, DRUMAir, LLC) (Creamean, 2017). The equipment was housed in a 47 x 35.7 x 17.6 cm case that included an inlet tube with a coarse metal filter. The case was attached to the railing of the ship located approximately 20 m above sea level and 8 m from the bow. It was positioned towards the front of the ship to avoid any possible contamination from the smoke stack. The DRUM impactor pumped in air at a rate of 28.6 L min^{-1} and was able to capture INPs by collecting aerosol particles at 4 different size ranges, (A) 0.15 – 0.34, (B) 0.34 – 1.21, (C) 1.21 – 2.96, and (D) 2.96 - > 12 µm. The particles were collected on a 20 x 190 x 0.05 mm strip of petrolatum-coated perfluoroalkoxy substrate (PFA) wrapped around a rotating drum 20 mm thick and 60 mm in diameter. Daily 24-hour aerosol samples promoted the sampling of rarer biological INPs and allowed continuous sampling during the entire cruise. The PFA strips were then cut, organized, and prepped to allow INP concentration analysis using drop freezing assay (DFA).

3.1.4 Drop-Freezing Assay

DFA is an immersion mode ice nucleation lab technique used to recreate cold cloud conditions similar to those found in nature. This analysis is able to test liquid samples on a cold plate apparatus and record how fast and what fraction of the sample froze as the temperature is lowered at a controlled rate. This technique takes use of previous but slightly modified apparati used in past INP investigations (Hill et al., 2016; Stopelli et al., 2014; Tobo, 2016; Wright and

Petters, 2013). The technique initiates by manually cleaning 50 mL beakers with isopropanol (99.5% ACS Grade, LabChem. Inc.) then placing them into a 6 L ultrasonic cleaner (model: P5-60A) for 30 minutes before baking at >150℃ for an additional 30 minutes. Once beakers were completely cleaned, the process deviates depending if the sample is sea water or aerosol. For sea water samples the process is relatively easy and includes transferring 2 mL of sea water sample into an individual beaker using a sterile, single-use syringe. If the sample was one of the daily aerosol samples, then 2 mL of molecular biology reagent water (MBR; 0.1 μm filtered) were added to an individual beaker and mixed with the PFA strip. The aerosol resuspension was then shaken at 500 rpm for 2 hours to guarantee complete resuspension (Bowers et al., 2009). Various copper disks measuring 76 mm in diameter and 3.2 mm in thickness were prepared by cleaning with isopropanol and adding a thin layer of petrolatum (100% Vaseline®) (Bowers et al., 2009; Tobo, 2016). This layer of petrolatum is added to create a hydrophobic layer, which keeps the spherical shape of the drops and creates a boundary between the drops and the metal to reduce any ice nucleation induced by the copper (Creamean, 2017; Creamean et al., 2018a; Hill et al., 2016).

Once the sea water or aerosol resuspension samples were transferred to the sterile beakers, using a new syringe, 0.25 mL of the sample was suctioned out and transferred to a prepared copper plate in the spiraling form of 100 individual drops creating an array of ~2.5 μL aliquots. Although manually creating 100 drops onto the copper plate can include human error and variance in drop volume, it was shown by Creamean et al. (2018b) that the syringe method is the most efficient way of running samples while also reducing the risk for contamination. Using a pipette would equalize drop volumes but would be too time consuming and result in too much air exposure during pipetting. Additionally, it has been proven that in order for differences in

drop volume to single handedly skew results, they would have to be orders of magnitude in difference (Bigg, 1953; Hader et al., 2014; Langham and Mason, 1958). The loaded copper plates were then transferred to a thermoelectric cold plate (Aldrich®) and covered with a plastic dome that had a tiny opening on the side. This opening was used to thread the thermometer probe that would then be inserted into the copper plate (Fig. 3.2).

The thermometer used was an Omega® thermometer/data logger (RDDXL4SD) with a 0.1 ℃ resolution and accuracy ±(0.4 % +1 ℃) for the K sensor types used (Creamean et al., 2018b). The thermometer was connected to a laptop that had in-house written software to log the time, temperature, and cooling rate of the analyzed samples. The temperature of the cold plate was then reduced and maintained at a cooling rate between 1-10 ℃ min^{-1} down from room temperature. Varying cooling rates have also not been found to significantly alter overall freezing temperatures (Vali and Stansbury, 1966; Wright and Petters, 2013). As the temperature dropped the observer was responsible for clicking the computer mouse as each single drop froze, and in doing so, capturing the temperature, cooling rate, and time of when that individual drop froze. The drops are visually detectable since unfrozen drops appear translucent and frozen drops turn a cloudy white. This process continues until the entire 100 drops are frozen or the cold plate reaches around -32 to -33 ℃ and the cooling rate is near zero.

Each sample was tested 3 times with 100 new drops each trial. At the end of each trial data existed in the form of text files that include the variables of temperature, cooling rate, fraction frozen, and percent of drop detection. Afterwards, triplicate results were binned every 0.5 ℃ to produce one freezing spectrum for each sample. Correspondingly, extensive testing by Dr. Creamean looking at the temperature difference between the center of the copper plate and the center of a liquid drop has shown that the drop is .33 ±0.15 ℃ warmer than the copper plate.

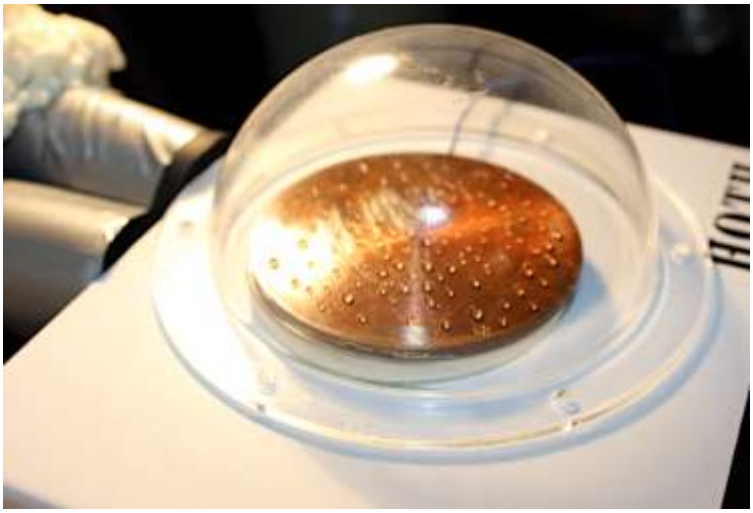

Figure 3.2: Photograph of a copper disk loaded with a liquid INP sample and placed on a cold plate. The thermometer probe that goes into the center of the copper disk looks like a thin blue wire and can be seen towards the back of the image. This sample in particular is prepped and ready to be frozen as part of the DFA methodology

This discrepancy is addressed by the inclusion of a +0.33 correction factor that is added to temperature measurements and 0.15 ℃ added to the probe accuracy uncertainty. For sea water samples only, a temperature correction of 2℃ was also applied to make up for the freezing point depression effect of salt in the samples. The validity of this technique is depicted by the ability to recreate same results with in error in all samples.

Although scientifically sound, it is important to be aware of some of the limitations of this technique. They include (1) detection of rarer INPs at specific temperatures during 1-2 of the tests or (2) uncertainties arising from instrumental artifacts, such as contamination during tests. By observing best lab practices, running each sample at least three times, and by always starting each test day by calibrating with blank MBR samples, we were able to lessen the impact of these uncertainties.

3.2 Testing Archaea as Ice Nucleating Particles

From the various quantifiable attributes still undiscovered in regards to archaea INPs, no lab cultured archaea species had ever been tested for their ice nucleating capabilities. This investigation appraised the first four archaea species to ever be tested for the immersion mode ice nucleating abilities. The four species analyzed are from the *Haloarchaea* class and were selected based on their ease of lab culturing and evidence supporting their presence in natural environments. The four species are: *Haloferax sulfurifontis* (haloferax), *Natronomonas pharaonsis* (natronomonas), *Haloquadratum walsbyi* (haloquadratum), and *Halococcus morrhuae* (halococcus).

***Haloferax sulfurifontis*:** Cells are non-motile, extremely pleomorphic, occurring mainly as irregularly shaped cells (1.0–1.5 μm in diameter), particularly during the stationary phase, and as rods (1.5– 1.7 x 0.5–0.6 μm), during the exponential growth phase. The genus *Haloferax*

requires relatively low salt concentrations compared to other haloarchaea genera (Elshahed et al., 2004; Oren, 2008).

***Natronomonas pharaonsis*:** A prokaryote found in solutions and soils up to pH 11 but thrives optimally in 3.5 M NaCl and at a pH of 8.5. Genome analysis suggests that it is adapted to cope with severe ammonia and heavy metal deficiencies that arise at high pH values. The cells are rod-shaped, 0.8 μm wide, and 2-3 μm long. Motile by flagella and a characteristic salmon pink color (Chaban et al., 2006; Ventosa, 2006).

***Haloquadratum walsbyi*:** A common species found in hypersaline waters and requires >14% (w/v) salt for growth. It has characteristic square cell shapes ~2 μm x 0.2 μm thickness, with the inclusion of gas vesicles. It thrives only in hypersaline solutions and can regularly represent > 80% of microbial population in these conditions (Dyall-Smith et al., 2011).

***Halococcus morrhuae*:** Found naturally in highly saline environments but also found in sea water. Non-motile aerobic microbe colonies have a red pigment and their cell walls differ significantly from the walls of most archaea in lacking typical constituents of peptidoglycan such as muramic acid or diamino- pimelic acid. Instead, their cell walls are 50 – 60 nm thick and are thought to be the main reason behind their resistance to lysing in dilute solution compared to other haloarchaea (Schleifer et al., 1982).

Production of extracellular polymeric substances (EPS) is a general property of microorganisms in natural environments and has been shown to occur both in prokaryotic (bacteria, archaea) and in eukaryotic (algae, fungi) microorganisms (Hoagland et al., 1993; Suresh-Kumar et al., 2007). EPS is composed of a variety of organic excretions including polysaccharides, proteins, nucleic acids, and amphiphilic compounds including (phospho) lipids (Poli et al., 2011). ESP play an important role in bacteria ice nucleation capable of increasing the

efficiency of live cells compared to inactive cells (Leck and Bigg, 2005; Tourney and Ngwengya, 2014; Zhang et al., 2012). By testing both an active (ESP producing) growing culture and an inactive (Non-ESP producing) stock culture of each species has allowed testing and comparison of all 4 haloarchaea and their respective EPS supplements.

Methodology for this investigation concurrently relied upon knowledge in microbiology, atmospheric chemistry, computer science, and laboratory procedures; resulting in a prime example of the interdisciplinary nature of environmental research. Execution of these methods were disseminated throughout four different locations, the College of Charleston (CofC), the University of Colorado at Boulder (UC Boulder), the University of Texas at El Paso (UTEP), and at the National Oceanic and Atmospheric Administration's (NOAA) Earth System Research Laboratory (ESRL) in Boulder, CO. Cultivation of microorganism solutions took place in South Carolina by Dr. Matthew E. Rhodes and his graduate student Lilyana Newman, followed by laboratory analysis at both ESRL and UC Boulder by Dr. Creamean and I, and then finally, computational analysis and report documentation performed at all institutions through a collaborative team effort.

3.2.1 Cultivation of Archaea Cultures

Media was prepared according to the recipes provided by the Leibniz-Institute DSMZ-German Collection of Microorganisms and Cell Cultures (DSMZ). Specifically, media 1019 was prepared for haloferax, media 1091 for haloquadratum, media 372 for halococcus, and media 371 for natronomonas. All strains were grown at 37˚ and shaken at 100 RPM until dense growth was observed. Purity of each culture was confirmed microscopically. Lysis assays were conducted by serially diluting actively growing culture with deionized water and performing cell counts. Actively growing cultures were then shipped overnight on ice from Charleston, SC to Boulder,

CO where an aliquot was used to inoculate fresh media. It was also observed that haloarchaea cells would lyse when mixed with non-saline aqueous solutions. With the exception of halococcus, the remaining three species would lyse into cell fragments instantaneously once suspended in MBR water.

3.2.2 Testing Conditions

Each of the species was tested for their ice nucleating abilities using DFA under various testing conditions. We wanted to test how each species would perform based on either a low or high archaea cell concentration and also contrast the performance of intact versus lysed cells. To accomplish this intact versus lysed comparison each species was diluted either in a 10% saline solution (intact) or MBR (lysed). Finally, to test the importance of archaeal ESP in archaea ice nucleating abilities, active growing samples were also tested. These active cultures would represent more natural conditions with cells at different life stages, consuming food and producing waste and EPS. For each these various testing conditions the archaea cell concentration was either low at 100X dilution or high at 10X dilution. These testing conditions resulted in a total of 23 archaea samples plus one blank MBR and one blank saline solution (Table 3.1). Since halococcus was identified to not lyse in MBR, only one active sample of halococcus was tested under the intact, high cell concentrations condition; the remaining archaea species had two active samples, one in MBR and the other in saline solution.

3.3 Remote Sensing Correlation between Plankton and Cloud Properties

This research portion of my thesis explores the possible link between satellite derived Chl-a concentrations and the seven aforementioned cloud variables over the Arctic Chukchi Sea. The Chukchi Sea during the summer is a great location for this type of study based on the current air temperature being 5˚ above the 1981 to 2010 average and generating some of the highest

Table 3.1: Indicates the 23 archaea samples prepared for ice nucleation analysis. The table does not include a blank MBR sample and a blank saline sample also analyzed.

Sample Number	Species	High (10X) or Low(100X) Cell Concentration	Intact or Lysed	Active or Inactive	Composition (mL)
1	*Haloferax*	High	Lysed	Inactive	MBR (1.8) + Archaea Stock (.2)
2	*Haloferax*	High	Intact	Inactive	Saline (1.8) + Archaea Stock (.2)
3	*Haloferax*	High	Intact	Active	Saline (1.8) + Active Culture (.2)
4	*Haloferax*	Low	Intact	Inactive	Saline (1.98) + Archaea Stock (.02)
5	*Haloferax*	Low	Intact	Inactive	Saline (1.98) + Archaea Stock (.02)
6	*Haloferax*	Low	Lysed	Active	MBR (1.98) + Active Culture (.02)
7	*Haloquadratum*	High	Lysed	Inactive	MBR (1.8) + Archaea Stock (.2)
8	*Haloquadratum*	High	Intact	Inactive	Saline (1.8) + Archaea Stock (.2)
9	*Haloquadratum*	High	Intact	Active	Saline (1.8) + Active Culture (.2)
10	*Haloquadratum*	Low	Intact	Inactive	Saline (1.98) + Archaea Stock (.02)
11	*Haloquadratum*	Low	Intact	Inactive	Saline (1.98) + Archaea Stock (.02)
12	*Haloquadratum*	Low	Lysed	Active	MBR (1.98) + Active Culture (.02)
13	*Natronomonas*	High	Lysed	Inactive	MBR (1.8) + Archaea Stock (.2)
14	*Natronomonas*	High	Intact	Inactive	Saline (1.8) + Archaea Stock (.2)
15	*Natronomonas*	High	Intact	Active	Saline (1.8) + Active Culture (.2)
16	*Natronomonas*	Low	Intact	Inactive	Saline (1.98) + Archaea Stock (.02)
17	*Natronomonas*	Low	Intact	Inactive	Saline (1.98) + Archaea Stock (.02)
18	*Natronomonas*	Low	Lysed	Active	MBR (1.98) + Active Culture (.02)
19	*Halococcus*	High	Lysed	Inactive	MBR (1.8) + Archaea Stock (.2)
20	*Halococcus*	High	Intact	Inactive	Saline (1.8) + Archaea Stock (.2)
21	*Halococcus*	High	Intact	Active	Saline (1.8) + Active Culture (.2)
22	*Halococcus*	Low	Intact	Inactive	Saline (1.98) + Archaea Stock (.02)
23	*Halococcus*	Low	Intact	Inactive	Saline (1.98) + Archaea Stock (.02)

concentrated phytoplankton biomass in the world. This spatial-temporal comparison explores the links at a monthly time scale using data images from the Moderate Resolution Imaging Spectroradiometer (MODIS) sensor on board NASA's Terra and Aqua satellites. Monthly images from 2003 to 2018 have created multiple time-series uncovering seasonal and multi-annual cycles of each natural variable. Correlation between time-series was also conducted helping reveal key cloud properties that are statistically correlated with variable chl concentrations.

3.3.1 Correlation Data and Methodology

MODIS provided all the necessary data to accomplish this remote sensing spatial-temporal analysis. Global Chl-a and cloud measurements have been available since 2002 as level-3 monthly products (Wan et al, 2002). The main motivation in choosing to work with monthly level-3 data is because it overcomes the hurdle of blotchy cloud activity creating data gaps in daily or 8-day images (Zhang et al, 2011. Instead, monthly level-3 products find the mean of each pixel in a month's time and results in a complete raster for cloud properties and a mostly complete raster for Chl-a (Moore et al, 2009). Chl-a data images still had some gaps due to persistent sea ice but monthly images are still a great improvement from daily images for this investigation's purpose.

Monthly data did not allow localized comparisons but instead facilitates a regional level comparison between the ocean and the atmosphere. Additionally, marine bioaerosol dispersal is not instantaneous so monthly data images can overcome this time-lag and better detect monthly, seasonal, and multi-annual links between environments. Finally, due to the surface of the water being covered by ice for most of the year, only monthly data images of June, July, and August for the years 2003 – 2018 were used. These months are typically those with low sea ice cover

compared to the rest of the year and provide the most spatially complete Chl-a rasters. Using data during months of low sea-ice cover will simultaneously help avoid the zenith distortion associated with cloud measurements at high latitudes. The zenith angle is the angle between a fixed latitude on Earth and the latitude of the Sun's declination. When the sun is low in the sky the effective path-length of the incoming solar beam through stratiform clouds, for example, is longer than when the sun is high in the sky. In harmony, a monthly time-scale using the months of June, July, and August will reduce zenith distortion and allow reliable measurements of the usually cloud covered sea surface during the Arctic summer.

The Chl-a concentration, OCI algorithm Global 4-km L3 satellite product was retrieved from the online data pool courtesy of the NASA Goddard Space Flight Center, Ocean Biology Processing Group, Aqua satellite Moderate Resolution Imaging Spectroradiometer (Aqua/MODIS), Greenbelt, MD, USA (https://oceancolor.gsfc.nasa.gov/) on 2018/08/05. The Terra/MODIS Aerosol Cloud Water Vapor Ozone Monthly L3 Global 1 Deg. CMG data set was acquired from the Level-1 and Atmosphere Archive & Distribution System (LAADS) Distributed Active Archiver Center (DAAC) also located in the Goddard Space Flight Center in Greenbelt, MD, USA (https://ladsweb.nascom.nasa.gov/) on 2018/09/14.

Chlorophyll concentration (mg m^{-3}) - The Aqua/MODIS monthly 4km resolution Chl-a data provides the surface concentration of Chl-a in milligrams of chlorophyll pigment per cubic meter (mg m^{-3}) at the ocean surface (Hu et al., 2012). Concentrations are calculated using an empirical relationship derived from in situ measurements of Chl-a and remote sensing reflectance ratios in the blue-to-green region of the visible spectrum between 440 and 670nm (Hu et al., 2012). Data were available and downloaded in scientific network common data format (NetCDF).

Table 3.2: Satellite data information from MODIS including marine surface Chl-a and eight optical and physical cloud properties. Data were obtained from NASA Goddard Space Flight Center https://oceancolor.gsfc.nasa.gov/)

Variable	Product	Temporal Resolution	Spatial Resolution	Reference
Chlorophyll-a Concentration (mg m^{-3})	MODIS_Terra_L3_Mo	Monthly	4 Km	Hu, C. et al., (2012)
Cloud Effective Radius Ice (μm)	MOD08_M3	Monthly	1 Degree (~ 111 Km)	Hubanks, Paul. et al., (2008)
Cirrus Reflectance (Unitless)	MOD08_M3	Monthly	1 Degree (~ 111 Km)	Hubanks, Paul. et al., (2008)
Cloud Top Temperature (K)	MOD08_M3	Monthly	1 Degree (~ 111 Km)	Hubanks, Paul. et al., (2008)
Cloud Top Pressure (hPa)	MOD08_M3	Monthly	1 Degree (~ 111 Km)	Hubanks, Paul. et al., (2008)
Cloud Effective Emissivity (W m^{-2})	MOD08_M3	Monthly	1 Degree (~ 111 Km)	Hubanks, Paul. et al., (2008)
Cloud Optical Thickness Ice (Unitless)	MOD08_M3	Monthly	1 Degree (~ 111 Km)	Hubanks, Paul. et al., (2008)
Cloud Water Path Ice Mean (g m^{-3})	MOD08_M3	Monthly	1 Degree (~ 111 Km)	Hubanks, Paul. et al., (2008)
Cloud Fraction Mean (Unitless)	MOD08_M3	Monthly	1 Degree (~ 111 Km)	Hubanks, Paul. et al., (2008)

Cloud properties - The Terra/MODIS Aerosol Cloud Water Vapor Ozone Monthly L3 Global 1Deg. CMG data set contains 1 x 1 degree grid average values of 800 atmospheric parameters related to atmospheric aerosol particle properties, total ozone burden, atmospheric water vapor, cloud optical and physical properties, and atmospheric stability indices (Hubanks et al., 2008). From the 800 parameters, eight physical and optical cloud variables were extracted for processing: cloud top temperature (K); cloud top pressure (hPa); cloud effective emissivity (W m^{-2}); ice cloud effective radius (μm); ice cloud mean water path (g m^{-3}); cirrus reflectance (unitless); ice cloud optical thickness (unitless); and mean cloud fraction (unitless) (Table 3.2). Data were available and downloaded in hierarchical data format (HDF).

The creation of a MATLAB® software programming script allowed the managing and processing of all 45 monthly satellite data images acquired. Four regions of interest were delineated for this remote sensing investigation (Figure 3.3). The largest of all regions is the Chukchi Sea region that spans a domain delineated by the most northwest coordinate (71° N, 179° W) and the southeastern coordinate (65° N, 160° W) covering the majority of the Chukchi Sea. The smaller three remaining areas of interest were based on visual detection of Chl-a "hot spots" that were repetitively apparent through the entire time-frame. These areas include: Kotzebue Sound (NW corner: 71° N, 179° W) (SE corner: 71° N, 179° W); Siberia Coast (NW corner: 71° N, 179° W) (SE corner: 71° N, 179° W); and Barrow Coast (NW corner: 71° N, 179° W) (SE corner: 71° N, 179° W) (Note: the city of Barrow is now named Utqiagvik, though for convenience the "Barrow Coast" name will be used here). These boundaries were not delineated based on any preexisting territorial extents and were solely based on visual detection. The script clips out any land areas in the cloud data allowing the discrete comparison between the marine Chl-a concentrations and marine clouds aloft. Next, a single average value was calculated from

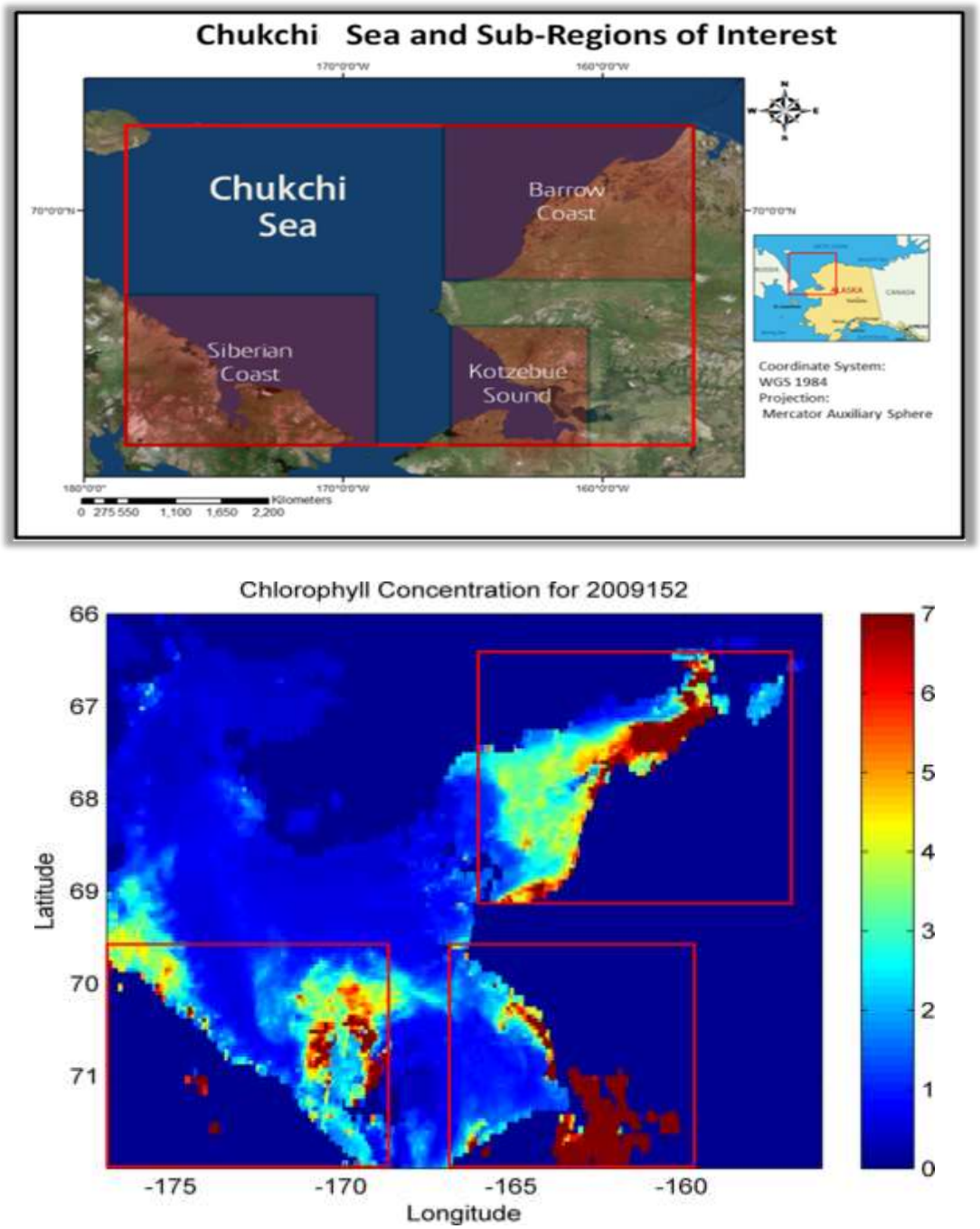

Figure 3.3: (top) Map of the Chukchi Sea. Red rectangles delineate the extent of my 4 regions of interest (ROI): the large "Chukchi Sea" ROI; sub-region "Siberian Coast"; sub-region "Kotzebue Sound"; and "Barrow Coast." (bottom) Monthly surface Chl-a concentrations in the Chukchi Sea that illustrate 3 biological "hot spots".

an entire monthly raster for each variable. In other words, all the pixels in a single monthly raster were averaged to produce that month's average value. This was done with both Chl-a and cloud variables. Furthermore, for seasonal and multi-annual comparison each June, July, and August ofeach year were averaged to obtain a summer average value. The summer season average vector files for each year were then plotted as time-series and were subsequently used in statistical comparison.

The various averaged summer time-series for both Chl-a and cloud variables were then correlated using the Pearson linear correlation coefficient to statistically measure the strength of the linear relationship between two paired natural variables (Gerten and Adrian, 2000; Prathumratana et al, 2008). Pearson's linear correlation coefficient is the most widely used linear correlation coefficient. For column X_a in matrix X and column Y_b in matrix Y, having means (1):

$$\overline{X}_a = \sum_{i=1}^{n} (X_{a,i})/n, \text{ and } \overline{Y}_b = \sum_{j=1}^{n} (X_{b,j})/n \quad (1)$$

Pearson's linear correlation coefficient *rho (a,b)* is defined as (2):

$$rho(a,b) = \frac{\sum_{i=1}^{n} (X_{a,i} - \overline{X}_a)(Y_{b,i} - \overline{Y}_b)}{\left\{ \sum_{i=1}^{n} (X_{a,i} - \overline{X}_a)^2 \sum_{j=1}^{n} (Y_{b,j} - \overline{Y}_b)^2 \right\}} \quad (2)$$

where n is the length of each column, X_a, Y_b are the individual sample points indexed with i and j respectively. Scatter plot linear fitting of the same data can then indicate a positive or negative correlation between paired variables. In tandem, these two analyses produced P- and R-values for all pair correlations. P-values below 0.05 depict a significant correlation with stronger

correlations close to 0.00. R-values indicate a positive or negative relationship and also indicate how well a linear model would fit the data.

4 Results

4.1 INARCO I/II Student Results

The combined interactions I experienced with researchers at NOAA ESRL and onboard *Healy* were an opportunistic experience that exposed me to different fields of study on a daily basis. During my summer internship at ESRL I received hands-on experience in a federal wet-lab setting exposing me to an assortment of professional and academic development opportunities within the NOAA workforce. Scientific training included working with aerosol samplers, meteorological stations, ice nucleation measurements, and protocols for aerosol and seawater sampling. Professional development included successfully participating in networking opportunities carried out by NOAA mentors and refining written and oral communication skills through presentation of research results. I gained mission-aligned core competencies evident by continued research partnerships between NOAA mentors and myself. Additionally, the NOAA-mission knowledge and skills learned allow me to contribute to a diverse and highly skilled candidate pool for future workforce of careers in disciplines that support the NOAA mission enterprise. Finally, the newly acquired competence I gained through this research has established invaluable early career networking opportunities that will leverage future educational and professional experiences.

Results of INARCO I are currently in submission for publication and will provide new insight into the oceanic and atmospheric processes that promote the production of marine INPs. INARCO II results are currently in the data analysis stage and are also expected to be published once results have been finalized. On the other hand, the results and personal outcomes from my summer student internship with NOAA and Dr. Jessie M. Creamean have provided me invaluable student research experience. Having had the opportunity to experience the daily life

of an Arctic researcher onboard *Healy* working as part of an interdisciplinary team has manifested as top-class field research experience. I gained experience collecting sediment from the ocean floor, investigating the marine benthic ecological and biological diversity, and examining water collected at multiple depths for chlorophyll concentrations. There were various onboard professional development opportunities like weekly talks from the PIs and on staging, dispatching, and collecting data with marine and atmospheric scientific equipment.

4.2 Archaea Results

All 23 archaea samples were analyzed successfully and allowed the calculation of average onset temperature (AOT) and fraction frozen freezing spectra for each sample. The AOT is the temperature when 1% of the sample is frozen, and although not exact, this is usually inferred to be the temperature when the first drop on the aliquot array froze. AOT is of scientific interest because while warmer temperature INPs are less abundant, they can individually initiate freezing in clouds. The AOT results are shown in Fig 4.1 and illustrate how all samples initiated freezing at temperatures warmer than that of homogeneous induced freezing, T >~ -38˚. The majority of INPs initiated ice nucleation between -20 and -30˚ with sample 12 (Intact active *Haloquadratum*, low concentration) having the warmest AOT at -9.97˚ For better distinction between samples overall fraction frozen, freezing spectra are of better use.

The fraction frozen spectra comparison between species can be examined in Fig. 4.2: (a) illustrates the freezing spectra of each species under intact-*low* cell concentration, while (b) illustrates the species under intact-*high* cell concentration. *Haloferax* and *Haloquadratum* both achieved a higher fraction frozen during low cell concentrations while *Halococcus* and *Natronomonas* experienced a higher fraction in high cell concentrations.

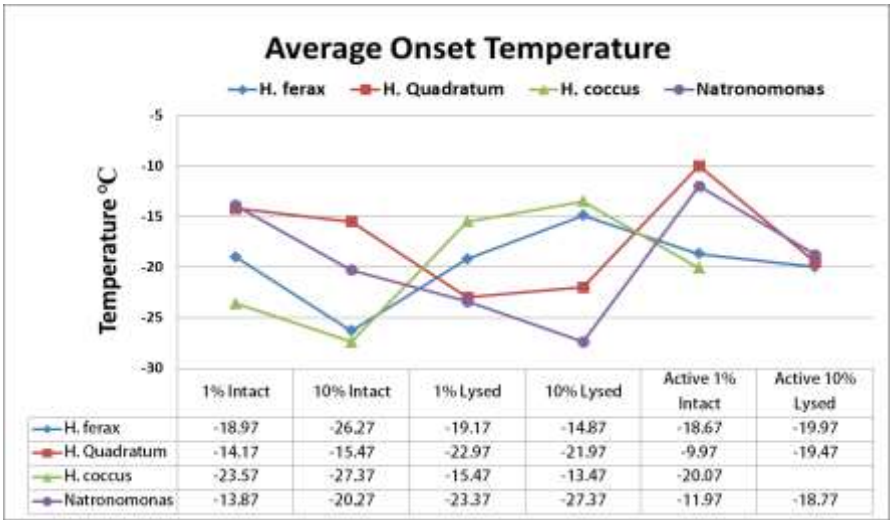

	1% Intact	10% Intact	1% Lysed	10% Lysed	Active 1% Intact	Active 10% Lysed
H. ferax	-18.97	-26.27	-19.17	-14.87	-18.67	-19.97
H. Quadratum	-14.17	-15.47	-22.97	-21.97	-9.97	-19.47
H. coccus	-23.57	-27.37	-15.47	-13.47	-20.07	
Natronomonas	-13.87	-20.27	-23.37	-27.37	-11.97	-18.77

Figure 4.1: Line graph illustrating average onset temperature of all 23 analyzed archaea species. The warmest average onset temperature was at T = 9.97℃ with inactive lysed *Haloquadratum* at low cell concentration.

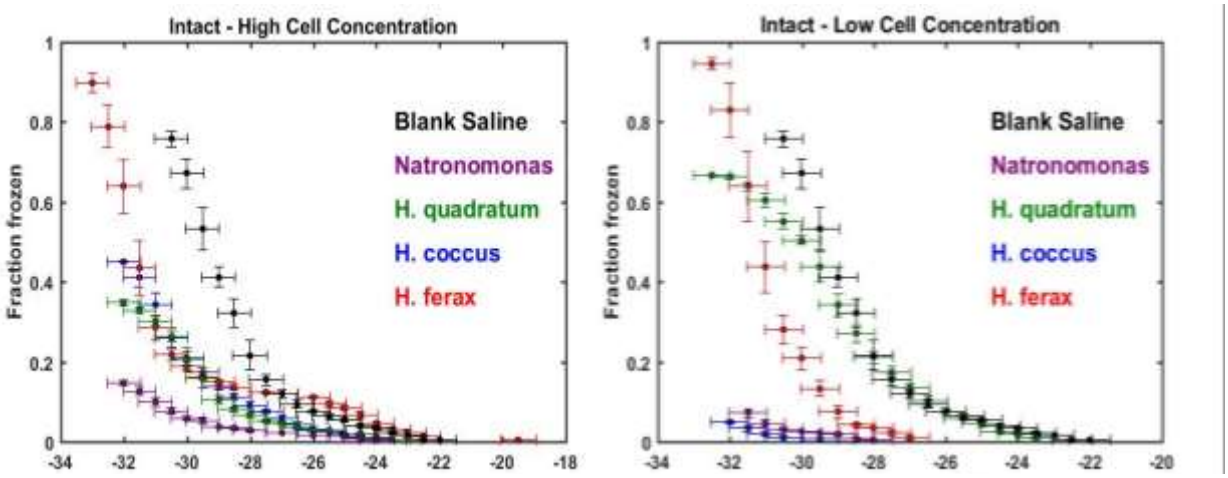

Figure 4.2: Fraction frozen spectra of the low versus high cell concentration comparison for each of the four *Haloarchae*a species.

Table 4.1: Results of the comparison between low (100x) and high (10x) cell concentrations between all four species.

Species	High (10X) or Low(100X) Cell Concentration	Intact or Lysed	Active or Inactive	Final Fraction Frozen
Haloferax	High	Intact	Inactive	.90
Haloferax	Low	Intact	Inactive	.92
Haloquadratum	High	Intact	Inactive	.35
Haloquadratum	Low	Intact	Inactive	.69
Haloccocus	High	Intact	Inactive	.48
Halococcus	Low	Intact	Inactive	.09
Natronomonas	High	Intact	Inactive	.15
Natronomonas	Low	Intact	Inactive	.10

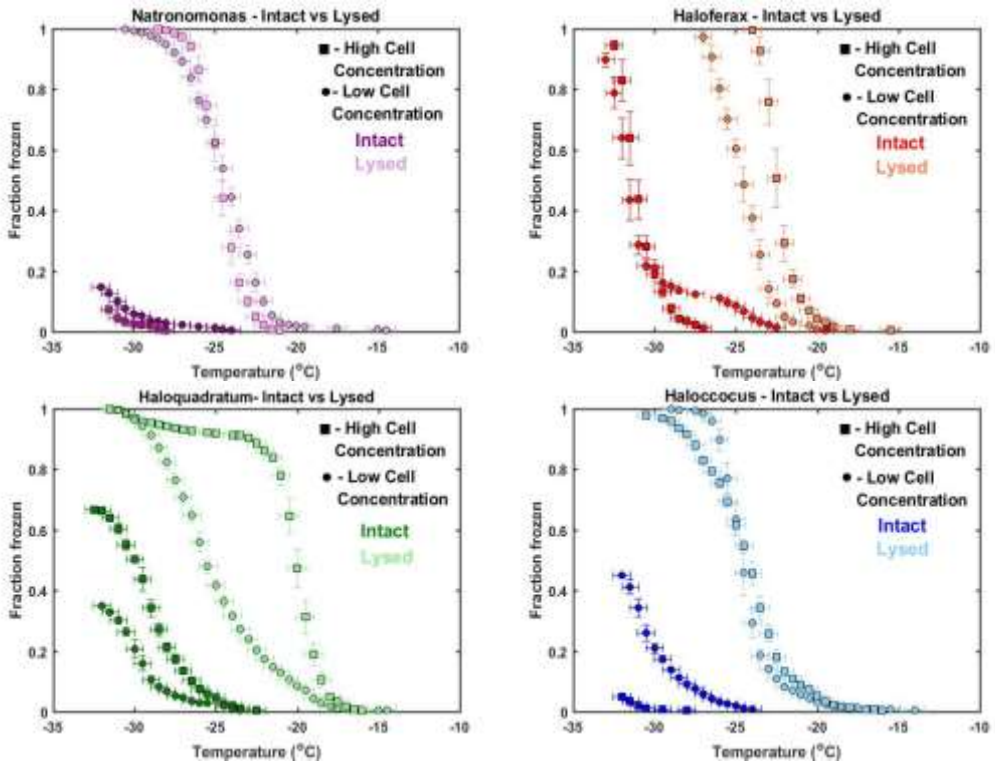

Figure 4.3: Fraction frozen spectra for each species comparing intact versus lysed archaea cells. The spectra also illustrate the difference between high and low cell concentration for both intact and lysed conditions.

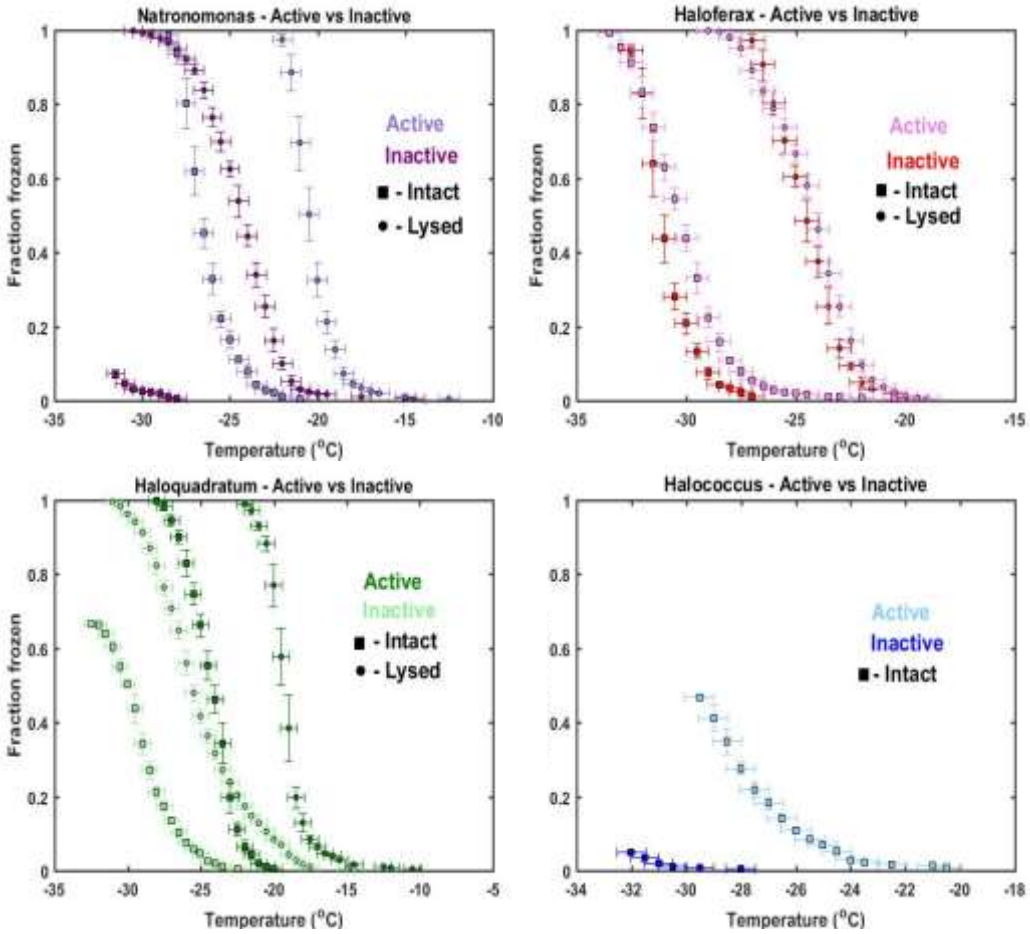

Figure 4.4: Fraction frozen spectra of each species comparing active (ESP producing) archaea cells versus inactive (Non-ESP producing) stock cells.

Final freeze fractions of each species are documented in Table 4.1 for these two testing conditions. All four species displayed unique comparisons but all shows signs of heterogeneous induced freezing by freezing above homogeneous induced freezing $T \leq \sim -38℃$.

Results from the intact versus lysed cell comparison can be seen in Fig. 4.3. Lysed cell samples reached 100% frozen, outperforming their intact counterpart in all four species. The lysed samples also all performed better compared to the blank MBR. These results illustrate what more natural atmospheric conditions these INPs might experience once they have left their hypersaline sources. The size of the cell fragments is unknown but it can be estimated to be a few orders of magnitude smaller than the intact archaeal cell.

In Fig. 4.4 the freezing spectra to compare inactive versus active samples is shown. The active samples were tested under two conditions (with the exception of *Halococcus*) and were plotted against their inactive counterpart with identical testing conditions. All active samples resulted with higher fraction frozen when compared to their inactive equivalent. All but *Halococcus* active samples reached 100% frozen at $T > -35℃$. The implications of active samples having improved ice nucleating capabilities indicates an important role in archaea EPS analogous to that of bacterial EPS.

4.3 Remote Sensing Analysis Results

Image processing analysis of monthly Chl-a satellite images from 2003 to 2018 for the months of June, July, and August resulted in the creation of several Chl-a time-series. Fig. 4.5 shows the Chl-a climatology of each region of interest by month and also by summer season.

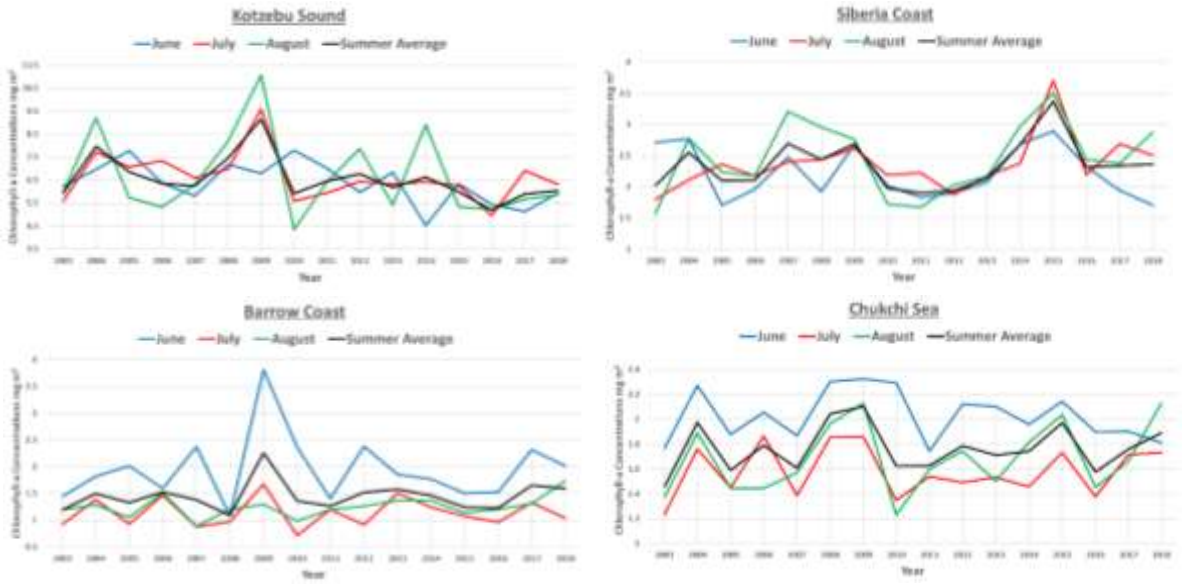

Figure 4.5: Time-series of the four regions of interest. Colored lines represent individual summer months since 2003 and the black line is the yearly summer average.

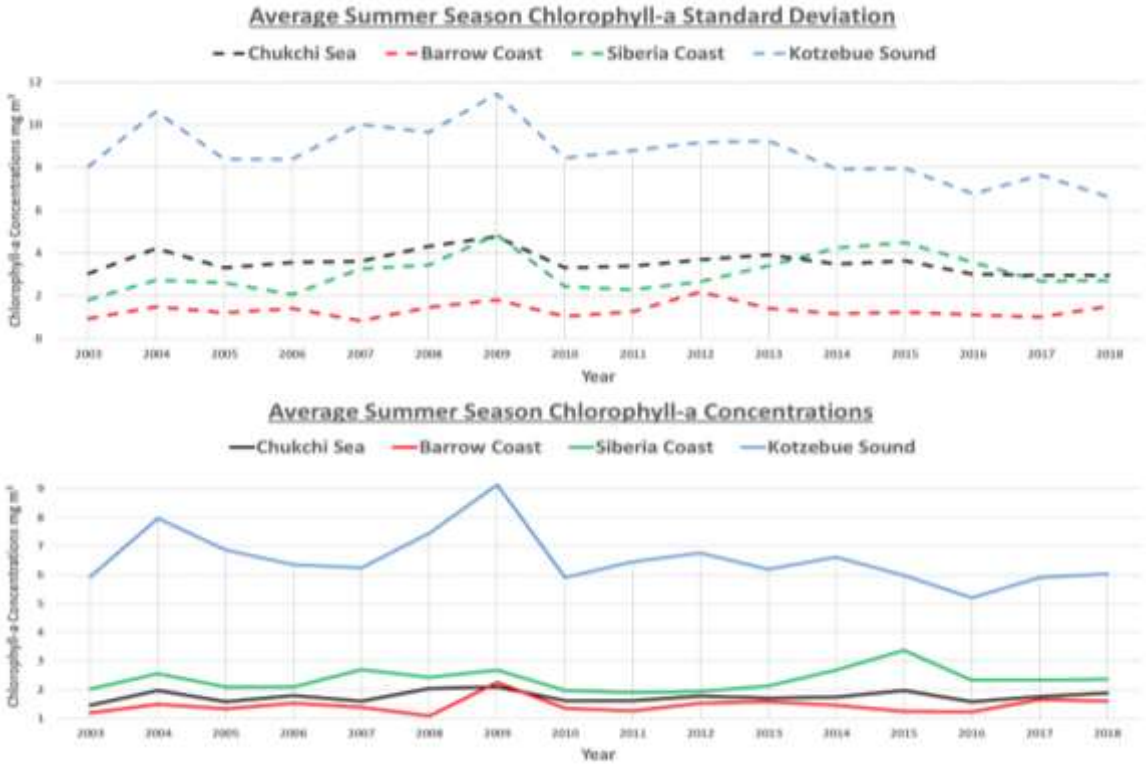

Figure 4.6: (top) Yearly summer Chl-a standard deviation plotted as a time-series for each region of interest. (bottom) Yearly summer Chl-a average concentrations plotted for each region of interest as time-series.

From the four regions of interest, Kotzebue Sound sustained the highest monthly and summer averaged concentrations of Chl-a ranging from 5.2 – 9.1 mg m^3. The other three regions' averaged monthly and summer concentrations remained lower in the range of 1.0 – 3.3 mg m^3. The month of June was prominent in producing dense concentrations of Chl-a over the large Chukchi Sea region and Barrow Coast sub-region. In the Kotzebue and Siberia Coast sub-regions, the distinctiveness between months was less noticeable with no large deviation between months. As a whole, the Chukchi Sea summer season has not experienced significant variation in Chl-a concentrations for the past 15 years and has remained stable with a linear fit slope of 0.0052. The year 2009 stood out as a year of exceptionally high concentrations found in all four regions marked by peaked Chl-a concentrations and elevated STD.

STD was related with increased of Chl-a concentrations through all four regions deduced to signify that as Chl-a increased the intensification was not experienced homogeneously but instead was heterogeneous in nature localized along continental coasts (Fig. 4.6). The explosion of life experienced here every summer is characterized by dense growth of phytoplankton near terrestrial coastlines associated with decreasing gradients in concentration leading to near zero in the open ocean. Blooms of Chl-a sometimes did appear further away from the coast but were ephemeral and probably created by an equally fleeting ocean and/or atmospheric process.

Time-series of cloud variables were also created and used for linear correlation. The Pearson linear correlations resulted in the creation of four correlation matrixes (Fig. 4.7 illustrates the correlation matrix for the largest Chukchi Sea region). The correlation matrix automatically correlates all variables between themselves, but this investigation is concentrated on the first column showing Chl-a correlations between Chl-a and the eight cloud variables of

Figure 4.7: Correlation matrix which utilizes Pearson linear correlation to perform paired variable correlations between chl and eight marine cloud variables over the Chukchi Sea.

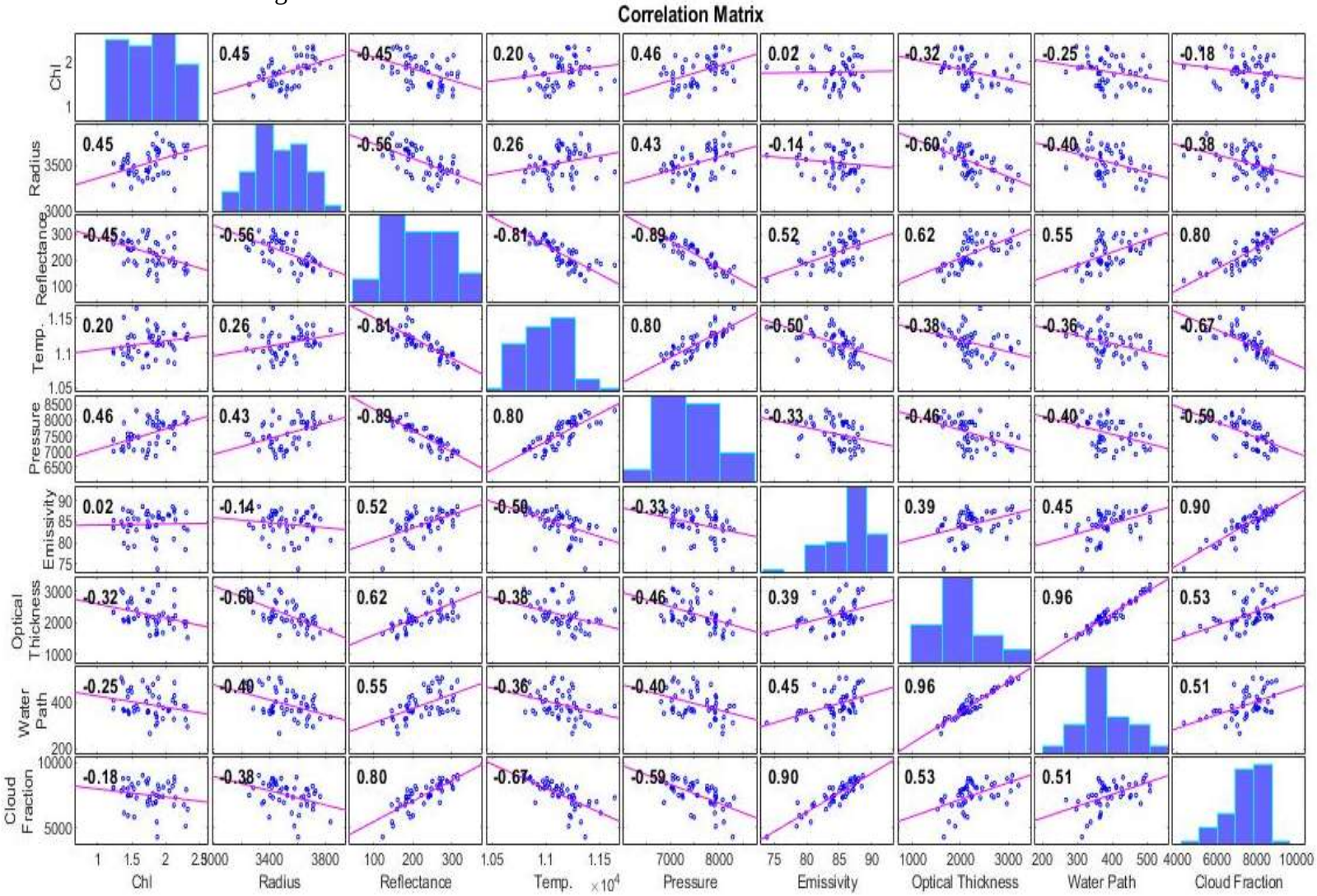

interest. The calculation of P-values for each correlation is also included in the matrix. Of the total 32 correlations at all 4 regions, seven had significant P-values <0.05. Scatter plots of each correlation were then executed to produce R^2 linear regression R-values. R-values indicate how well a linear regression fits the data and its reliability in forecasting any trends. All P- and R-values are shown in Table 4.2.

The largest region, the Chukchi Sea, had the highest percentage of significant correlations with four noteworthy results: ice cloud effective radius (P-value = 0.0013, R-value = 0.45); cirrus reflectance (P-value = 0.0013, R-value = -0.045); cloud top pressure (P-value = 0.0009, R-value = 0.45); and ice cloud optical thickness (P-value = 0.0267, R-value = -0.32) (Figure 4.). From the smaller three sub-regions Barrow Coast was the only one to produce three additional noteworthy correlations: cirrus reflectance (P-value = 0.0002, R-value = -0.52); cloud top pressure (P-value = 0.0018, R-value = 0.44); cloud fraction mean (P-value = 0.005, R-value = 0.40). The remaining two sub-regions did not produce any statistically significant correlations most likely due to the combined effect of a smaller area and course spatial resolution cloud data.

At the regional scale the significant positive correlations between Chl-a with ice cloud effective radius and cloud top pressure have shown that a change in surface Chl-a has the potential to directly affect the density of cloud ice and cloud top height. An increase in Chl-a concentrations from 1.2 to 2.2 mg m^3 has been correlated (P-value, 0.0013) to increase ice cloud effective radius from 3400 to 3600 μm and cloud top pressure (P-value, 0.0009) from 7100 to 7900 hPa. Regional negative correlations indicate that an increase in Chl-a concentrations from 1.2 to 2.2 mg m^3 are correlated (P-value, 0.0013) to decreased cirrus cloud reflectance (MODIS channel 1.38-μm) from 275 to 200 and ice cloud optical thickness (P-value, 0.0267) (MODIS channel 0.858-μm) from 2400 to 2000 (Fig. 4.8).

Table 4.2: Results of the remote sensing correlation analysis between chl and eight optical and physical cloud variables. Both p- and R-values are documented for each paired correlation for each of the four regions of interest.

	Ice Cloud Effective Radius		*Cirrus Reflectance*		*Cloud Top Temperature*		*Cloud Top Pressure*	
Chl-a Concentration	R-Value	P-Value	R-Value	P-Value	R-Value	P-Value	R-Value	P-Value
Chukchi Sea	0.45	0.0013	-0.45	0.0013	0.20	0.1178	0.46	0.0009
Barrow Sound	0.12	0.4069	-0.52	0.0002	0.18	0.2121	0.44	0.0018
Siberian Coast	-0.20	0.1835	0.06	0.6748	0.08	0.5994	0.04	0.7617
Kotzebue Sound	-0.22	0.1274	-0.01	0.9657	0.00	0.9844	-0.04	0.8054

	Cloud Effective Emissivity		**Ice Cloud Optical Thickness**		**Ice Cloud Water Path**		**Cloud Fraction**	
Chl-a Concentration	R-Value	P-Value	R-Value	P-Value	R-Value	P-Value	R-Value	P-Value
Chukchi Sea	0.02	0.9743	-0.32	0.0267	-0.25	0.0925	-0.18	0.2162
Barrow Sound	-0.10	0.5006	-0.02	0.8974	0.06	0.6747	-0.40	0.0050
Siberian Coast	-0.04	0.7962	0.11	0.4761	0.05	0.7373	0.04	0.8110
Kotzebue Sound	-0.18	0.2290	0.08	0.5931	0.07	0.6431	-0.14	0.3360

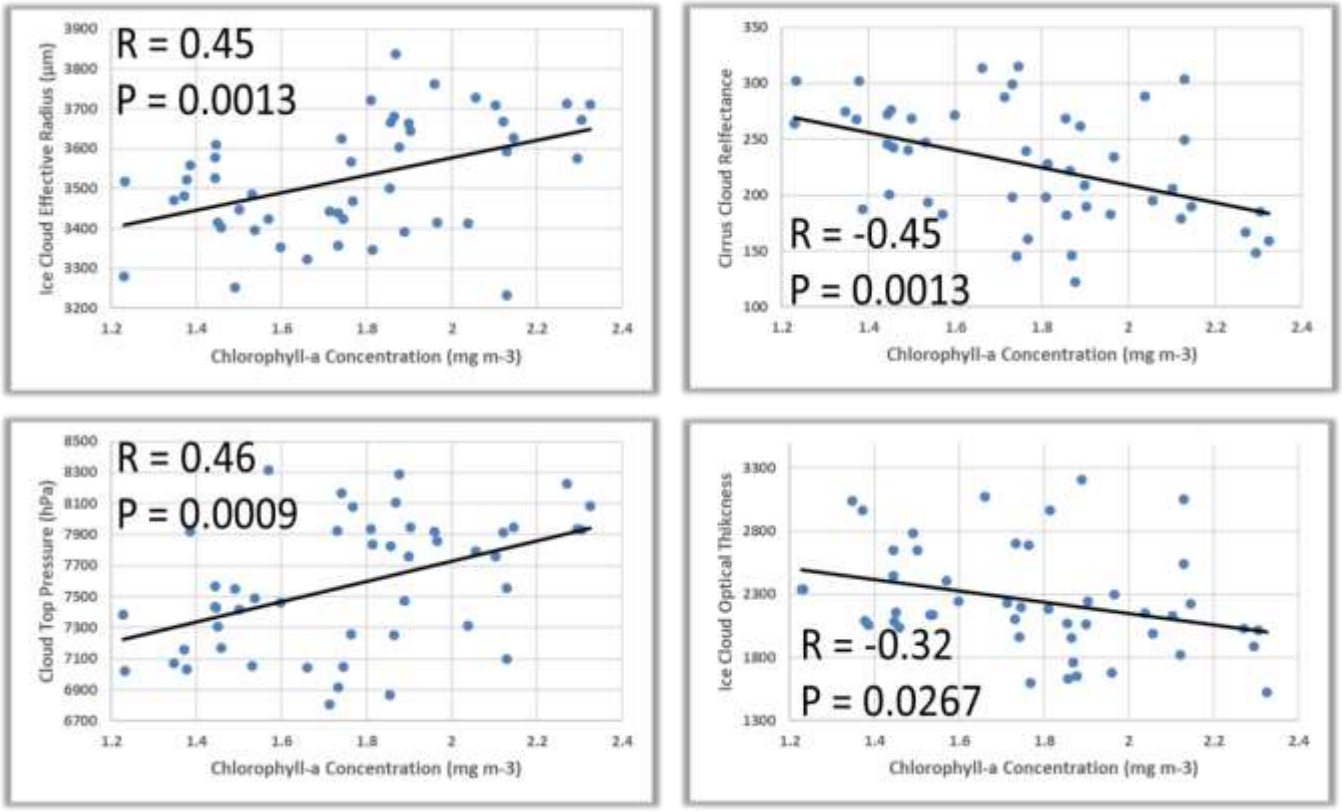

Figure 4.8: Scatter plots of the four statistically correlated paired variables in the larger Chukchi Sea region of interest. R^2 linear regression allowed the calculation of R-value for each correlation.

5 Conclusion and Implications

This research has provided further evidence for an interconnected Arctic system between the atmosphere and the ocean which involves the emission of millions of marine INPs into the atmosphere. INARCO I/II field campaigns have allowed the physical sampling of both marine and atmospheric environments for direct evidence of a permeable ocean-air interface. Although results of the investigations are not yet published, it is certain that the results of the analyses of all Arctic air and sea water samples will undoubtedly improve parameterization and quantification of marine INPs in this region. INARCO I/II are the start of a multi-annual investigation that hopes to not only understand where Arctic marine INPs are located but understand how concentrations change through time. INARCO III is currently scheduled for October 2019.

The archaea ice nucleating analysis has demonstrated that intact, lysed, active, and inactive archaea cells are all capable of ice nucleation above homogeneous freezing. These results are of great implication since no archaea species had ever been tested for immersion mode freezing capabilities. This is the start of parameterization for the entire archaea domain and results all indicate some form ice nucleating ability at $T \geq -35℃$. Results have shown ice nucleation possible as warm as -9.97 ℃ signifying a very important source of ice nucleation in air absent from dust or other bioaerosols. This natural forcing is currently inadequately incorporated into atmospheric models and justifies the need for further archaeal INP research. Archaea are also relevant climatic forces in paleo-climatic models when Earth was dominated by only bacteria, archaea, and other prokaryotes. Their ubiquitous presence in Earth's current biosphere warrants additional research into archaea ice nucleation abilities. Testing haloarchaea has presented unique difficulties including the freezing suppression of salt in the samples.

From the remote sensing analysis only seven correlations were deemed statistically significant. It is suggested that the lack of correlations, especially in the smaller –sub-regions, is due to coarse cloud data spatial resolution. Correlation results appear to improve with region size increase so this type of analysis is recommended for regional scale investigations until cloud images spatial resolution are improved. Additionally, isolating the effect of marine INPs on the marine clouds can be enhanced by identifying months or events of increased long-range dust transport into this area, allowing the exclusion of these months from the dataset and producing more accurate marine INP representation.

Although this remote sensing analysis does not explain the physical and chemical processes leading to the statistically correlations, it does identify the long-term links between surface Chl-a concentrations and certain cloud variable. The four regional correlations explained in sub-section 4.3 indicate that as Chl-a concentrations increase across the Chukchi Sea, the marine clouds appear to rise in elevation, become less dense, increase in ice crystal size, and become less bright. Further research is needed to understand what forces are leading to these changes, but it is hypothesized these reactions can be explained by the release of latent heat when a water droplet changes phase into ice. Latent heat could provide enough propulsion for the cloud to expand further up into the atmosphere and subsequently become less dense. The increase in ice cloud effective radius would also be justified by this hypothesis since an ice crystal is many times larger than a water droplet. An increased availability of marine INPs during the Chukchi summer could be the main force providing the INP necessary to kick start this phase change in marine clouds.

Interestingly, the summer average Chl-a concentration for the Chukchi Sea did not have a significant increase in the past 15 years. This is surprising since it was first thought that a large

increase in air temperature would encourage equally high Chl-a concentrations. Since 2003 the Chukchi Sea has maintained remarkably high concentrations in surface Chl-a and it is possible that since the sea has always sustained high concentrations then increased air temperature would not have such a pronounced effect. The effect of increasing air temperature, on the contrary, might be very marked in a different region which has not historically been an exceptionally high phytoplankton producer.

Assimilation of results of this study exemplifies the importance of considering plankton biomass in future climatic models since changes in biological sea processes are capable of influencing cloud properties and subsequently the surface radiation budget. This research has provided some modeling parameterization but further studies are still required to obtain the data needed for accurate modeling. Together this multi-method approach to an environmental question has provided support for continued uses of this research format. Although similar to multi-disciplinary, I believe the term multi-method is better representative of this investigation since it focused and was developed to identify relevant scientific perspectives that ended up being naturally multi-disciplinary.

Overall, this thesis research has allowed a better understanding of the Arctic links between plankton biomass, atmospheric INPs, and their subsequent effect on clouds. Field research has proven the fact that marine INP sources are dictated and produced by the combined forces of ocean and atmospheric process. Lab analysis has proven that archaea microorganisms do in fact have the potential to be biogenic INP sources found in nature. Lastly, remote sensing analysis provided evidence for Arctic clouds in the Chukchi Sea to be directly affected by the concentration of surface marine Chl-a concentrations below. Results call for future investigations that would allow a detailed quantification for the now recognized links. The

dynamic Arctic continues to change in ways we haven't anticipated, and it is our scientific and human responsibility to gain a good understanding not only for forecasting, but to also limit the human impact and mitigate our effect to guarantee a sustainable world for future generations.

References

Abbatt, J. P. D, and 69 others. 2019. New insights into aerosol and climate in the Arctic. *Atmospheric Chemistry and Physics*, 19, 2527-2560.

Abbatt, J. P. D., Benz, S., Cziczo, D. J., Kanji, Z., Lohmann, U., & Möhler, O. 2006. Solid ammonium sulfate aerosols as ice nuclei: A pathway for cirrus cloud formation. *Science*, 313 (5794), 1770-1773.

Agawin, N. S., Duarte, C. M., & Agustí, S. 2000. Nutrient and temperature control of the contribution of picoplankton to phytoplankton biomass and production. *Limnology and Oceanography*, 45 (3), 591-600.

Akila, M., Priyamvada, H., Ravikrishna, R., & Gunthe, S. S. 2018. Characterization of bacterial diversity and ice-nucleating ability during different monsoon seasons over a southern tropical Indian region. *Atmospheric Environment*, 191, 387-394.

Alpert, P. A., Aller, J. Y., & Knopf, D. A. 2011. Ice nucleation from aqueous NaCl droplets with and without marine diatoms. *Atmospheric Chemistry and Physics*, 11 (12), 5539-5555.

Anand, N., Satheesh, S. K., & Moorthy, K. K. 2017. Dependence of atmospheric refractive index structure parameter (Cn^2) on the residence time and vertical distribution of aerosols. *Optics Letters*, 42 (14), 2714-2717.

Ardyna, M., Babin, M., Devred, E., Forest, A., Gosselin, M., Raimbault, P., & Tremblay, J. É. 2017. Shelf-basin gradients shape ecological phytoplankton niches and community composition in the coastal Arctic Ocean (Beaufort Sea). *Limnology and Oceanography*, 62 (5), 2113-2132.

Arrigo, K. R., Perovich, D. K., Pickart, R. S., Brown, Z. W., Van Dijken, G. L., Lowry, K. E., Mills, M. M., Palmer, M. A., Balch, W. M., Bahr, F., & Bates, N. R. 2012. Massive phytoplankton blooms under Arctic sea ice. *Science*, 336 (6087), 1408-1408.

Arrigo, K. R., Perovich, D. K., Pickart, R. S., Brown, Z. W., Van Dijken, G. L., Lowry, K. E., Mills, M. M., Palmer, M. A., Balch, W. M., Bates, N. R., & Benitez-Nelson, C. R. 2014. Phytoplankton blooms beneath the sea ice in the Chukchi Sea. *Topical Studies in Oceanography*, 105, 1-16.

Atlas okeanov. Severnyi Ledovityi okean (Atlas of Oceans. The Arctic Ocean), Leningrad: GUNiO MO SSSR, 1980.

Augustin, S., Wex, H., Niedermeier, D., Pummer, B., Grothe, H., Hartmann, S., Tomsche, L., Clauss, T., Voigtländer, J., Ignatius, K., & Stratmann, F. 2013. Immersion freezing of birch pollen washing water. *Atmospheric Chemistry and Physics*, 13 (21), 10989-11003.

Ault, A. P., Moffet, R. C., Baltrusaitis, J., Collins, D. B., Ruppel, M. J., Cuadra-Rodriguez, L. A., Zhao, D., Guasco, T. L., Ebben, C. J., Geiger, F. M., & Bertram T.H. 2013. Size-dependent changes in sea spray aerosol composition and properties with different seawater conditions. *Environmental Science & Technology*, 47 (11), 5603-5612.

Baddock, M. C., Mockford, T., Bullard, J. E., & Thorsteinsson, T. 2017. Pathways of high-latitude dust in the North Atlantic. *Earth and Planetary Science Letters*, 459, 170-182.

Baker-Austin, C. & Dopson, M. 2007. Life in acid: pH homeostasis in acidophiles. *Trends in Microbiology*, 15 (4), 165-171.

Barahona, D., Molod, A., & Kalesse, H. 2017. Direct estimation of the global distribution of vertical velocity within cirrus clouds. *Scientific Reports*, 7 (1), 6840.

Barthel, S., Tegen, I., & Wolke, R. 2019. Do new sea spray aerosol source functions improve the results of a regional aerosol model? *Atmospheric Environment*, 198, 265-278.

Bauer, H., Giebl, H., Hitzenberger, R., Kasper-Giebl, A., Reischl, G., Zibuschka, F., & Puxbaum, H. 2003. Airborne bacteria as cloud condensation nuclei. *Journal of Geophysical Research: Atmospheres*, 108 (D21), 4658, doi:10.1029/2003JD003545.

Baumgardner, D., Abel, S. J., Axisa, D., Cotton, R., Crosier, J., Field, P., Gurganus, C., Heymsfield, A., Korolev, A., Kraemer, M., & Lawson, P. 2017. Cloud ice properties: in situ measurement challenges. *Meteorological Monographs*, 58, 9-1- 9.23.

Bigg, E. K. 1953. The supercooling of water. *Proceedings of the Physical Society B*, 66 (8), 688-694.

Blanchard-Wrigglesworth, E., Barthélemy, A., Chevallier, M., Cullather, R., Fučkar, N., Massonnet, F., Posey, P., Wang, W., Zhang, J., Ardilouze, C., & Bitz, C. M. 2017. Multi-model seasonal forecast of Arctic sea-ice: forecast uncertainty at pan-Arctic and regional scales. *Climate Dynamics*, 49 (4), 1399-1410.

Bluhm, B. A., Swadling, K. M., & Gradinger, R. 2017. Sea ice as a habitat for macrograzers. In: Thomas, D.N. (Ed.) *Sea Ice* (3rd ed.), Wiley: Chichester, pp. 394-414.

Blunden, J. & Arndt, D.S. 2016. State of the climate in 2015. *Bulletin of the American Meteorological Society*, 97 (8), S1-S275. doi:10.1175/2016BAMSStateoftheClimate.1

Boeke, R. C. & Taylor, P. C. 2018. Seasonal energy exchange in sea ice retreat regions contributes to differences in projected Arctic warming. *Nature Communications*, 9 (1), 5017.

Boucher, O. 2015. Atmospheric Aerosols. In: Boucher, O. (Ed.), *Atmospheric Aerosols*, Springer: Dordrecht, pp. 9- 24.

Bowers, R.M., Lauber, C.L., Wiedinmyer, C., Hamady, M., Hallar, A.G., Fall, R., Knight, R. & Fierer, N. 2009. Characterization of airborne microbial communities at a high-elevation site and their potential to act as atmospheric ice nuclei. *Applied and Environmental Microbiology*, 75(15), 5121-5130.

Boyer, T. P., Levitus, S., Antonov, J. I., Locarnini, R. A., & Garcia, H. E. 2005. Linear trends in salinity for the world ocean, 1955–1998, *Geophysical Research Letters*, 32, L01604, doi:10.1029/2004GL021791.

Brooks, S. D. & Thornton, D. C. 2018. Marine aerosols and clouds. *Annual Review of Marine Science*, 10, 289-313.

Calvo, A. I., Alves, C., Castro, A., Pont, V., Vicente, A. M., & Fraile, R. 2013. Research on aerosol sources and chemical composition: past, current and emerging issues. *Atmospheric Research*, 120, 1-28.

Carton, J. A., Ding, Y., & Arrigo, K. R. 2015. The seasonal cycle of the Arctic Ocean under climate change. *Geophysical Research Letters*, 42 (18), 7681-7686.

Chaban, B., Ng, S.Y., & Jarrell, K. F. 2006. Archaeal habitats—from the extreme to the ordinary. *Canadian Journal of Microbiology*, 52 (2), 73-116.

Chapin, F. S., Sommerkorn, M., Robards, M. D., & Hillmer-Pegram, K. 2015. Ecosystem stewardship: a resilience framework for arctic conservation. *Global Environmental Change*, 34, 207-217.

Charlson, R. J., Lovelock, J. E., Andreae, M. O. & Warren, S.G. 1987. Oceanic phytoplankton, atmospheric sulphur, cloud albedo and climate. *Nature*, 326 (6114), 655-661.

Choudoir, M. J., Barberán, A., Menninger, H. L., Dunn, R. R., & Fierer, N. 2018. Variation in range size and dispersal capabilities of microbial taxa. *Ecology*, 99 (2), 322-334.

Cimoli, E., Lucieer, A., Meiners, K. M., Lund-Hansen, L. C., Kennedy, F., Martin, A., McMinn, A., & Lucieer, V. 2017. Towards improved estimates of sea-ice algal biomass:

experimental assessment of hyperspectral imaging cameras for under-ice studies. *Annals of Glaciology*, 58 (75), 68-77.

Cochran, R. E., Ryder, O. S., Grassian, V. H., & Prather, K. A. 2017. Sea spray aerosol: The chemical link between the oceans, atmosphere, and climate. *Accounts of Chemical Research*, 50 (3), 599-604.

Collier, K. N. & Brooks, S. D. 2016. Role of organic hydrocarbons in atmospheric ice formation via contact freezing. *The Journal of Physical Chemistry*, 120 (51), 10169-10180.

Coluzza, I., Creamean, J., Rossi, M., Wex, H., Alpert, P., Bianco, V., Boose, Y., Dellago, C., Felgitsch, L., Fröhlich-Nowoisky, J., & Herrmann, H. 2017. Perspectives on the future of ice nucleation research: research needs and unanswered questions identified from two international workshops. *Atmosphere*, 8 (8), 138.

Conen, F. & Yakutin, M. V. 2018. Soils rich in biological ice-nucleating particles abound in ice-nucleating macromolecules likely produced by fungi. *Biogeosciences*, 15 (14), 4381-4385.

Coopman, Q., Riedi, J., Finch, D. P., & Garrett, T. J. 2018. Evidence for changes in Arctic cloud phase due to long-range pollution transport. *Geophysical Research Letters*, 45 (19), 10709- 10718.

Courtney, M. B., Scanlon, B. S., Rikardsen, A. H., & Seitz, A. C. 2016. Marine behavior and dispersal of an important subsistence fish in Arctic Alaska, the Dolly Varden. *Environmental Biology of Fishes*, 99 (3), 209-222.

Creamean, J. M. 2017. Exploratory ice nucleation measurements at Oliktok field campaign report, U.S. Department of Energy, Office of Science, Office of Biological and Environmental Research (No.DOE/SC-ARM-17-034). DOE Office of Science Atmospheric Radiation Measurement (ARM) Program (United States); Pacific Northwest National Lab.(PNNL), Richland, WA (United States).

Creamean, J. M., Primm, K. M., Tolbert, M. A., Hall, E. G., Wendell, J., Jordan, A., Sheridan, P. J., Smith, J., & Schnell, R. C. 2018a. HOVERCAT: a novel aerial system for evaluation of aerosol–cloud interactions. *Atmospheric Measurement Techniques*, 11, 3969-3985, https://doi.org/10.5194/amt-11-3969-2018, 2018.

Creamean, J. M., Mignani, C., Bukowiecki, N., & Conen, F. 2018b. Using spectra characteristics to identify ice nucleating particle populations during winter storms in the Alps. *Atmospheric Chemistry and Physics Discussions*, https://doi.org/10.5194/acp-2018-1082.

Creamean, J.M., Cross, J.N., Pickart, R.S., McRaven, L., Lin, P., Pacini, A., Hanlon, R., Schmale, D.G., Ceniceros, J., Aydell, T., Colombi, N., Bolger, E., & DeMott, P.J. Submitted. Ice nucleating particles carried from below a phytoplankton bloom to the Arctic atmosphere. *Nature Communications*, submitted.

Curry, J.A. 1995. Interactions among aerosols, clouds, and climate of the Arctic Ocean. *Science of the Total Environment*, 160, 777-791.

Curry, J. A., Schramm, J. L., Rossow, W. B., & Randall, D. 1996. Overview of Arctic cloud and radiation characteristics. *Journal of Climate*, 9 (8), 1731-1764.

Cziczo, D. J., Ladino, L., Boose, Y., Kanji, Z. A., Kupiszewski, P., Lance, S., Mertes, S., & Wex, H. 2017. Measurements of ice nucleating particles and ice residuals. *Meteorological Monographs*, 58, 8-1 – 8-13.

Danielson, S. L., Eisner, L., Ladd, C., Mordy, C., Sousa, L., & Weingartner, T. J. 2017. A comparison between late summer 2012 and 2013 water masses, macronutrients, and

phytoplankton standing crops in the northern Bering and Chukchi Seas. *Topical Studies in Oceanography*, 135, 7-26.

Deming, J. W. & Collins, R. E. 2017. Sea ice as a habitat for bacteria, archaea and viruses. In: Thomas, D.N. (Ed.) *Sea Ice* (3rd ed.), Wiley: Chichester, pp. 326-351.

DeMott, P. J., Prenni, A. J., Liu, X., Kreidenweis, S. M., Petters, M. D., Twohy, C. H., Richardson, M. S., Eidhammer, T., & Rogers, D. C. 2010. Predicting global atmospheric ice nuclei distributions and their impacts on climate. *Proceedings of the National Academy of Sciences (USA)*, 107, 11217-11222.

DeMott, P. J., Hill, T. C., McCluskey, C. S., Prather, K. A., Collins, D. B., Sullivan, R. C., Ruppel, M. J., Mason, R. H., Irish, V. E., Lee, T., & Hwang, C. Y. 2016. Sea spray aerosol as a unique source of ice nucleating particles. *Proceedings of the National Academy of Sciences (USA)*, 113 (21), 5797-5803.

Dentener, F., Drevet, J., Lamarque, J. F., Bey, I., Eickhout, B., Fiore, A. M., Hauglustaine, D., Horowitz, L. W., Krol, M., Kulshrestha, U. C., & Lawrence, M. 2006. Nitrogen and sulfur deposition on regional and global scales: A multimodel evaluation. *Global Biogeochemical Cycles*, 20 (4), GB4003, doi:10.1029/2005GB002672

Després, V., Huffman, J. A., Burrows, S. M., Hoose, C., Safatov, A., Buryak, G., Fröhlich-Nowoisky, J., Elbert, W., Andreae, M., Poeschl, U., & Jaenicke, R. 2012. Primary biological aerosol particles in the atmosphere: a review. *Tellus B: Chemical and Physical Meteorology*, 64:1, 15598, DOI: 10.3402/ tellusb.v64i0.1559

Doney, S. C., Ruckelshaus, M., Duffy, J. E., Barry, J. P., Chan, F., English, C. A., Galindo, H. M., Grebmeier, J. M., Hollowed, A. B., Knowlton, N., & Polovina, J. 2012. Climate change impacts on marine ecosystems. *Annual Review of Marine Science*, 4, 11-37.

Du, R., Du, P., Lu, Z., Ren, W., Liang, Z., Qin, S., Li, Z., Wang, Y., & Fu, P. 2017. Evidence for a missing source of efficient ice nuclei. *Scientific Reports*, 7, 39673.

Durack, P. J., Wijffels, S. E., & Matear, R. J. 2012. Ocean salinities reveal strong global water cycle intensification during 1950 to 2000. *Science*, 336 (6080), 455-458.

Dyall-Smith, M. L., Pfeiffer, F., Klee, K., Palm, P., Gross, K., Schuster, S. C., Rampp, M. & Oesterhelt, D. 2011. Haloquadratum walsbyi: limited diversity in a global pond. *PLOS One*, *6*(6), 209.

Elshahed, M. S., Savage, K. N., Oren, A., Gutierrez, M. C., Ventosa, A., & Krumholz, L. R. 2004. Haloferax sulfurifontis, a halophilic archaeon isolated from a sulfide-and sulfur-rich spring. *International Journal of Systematic and Evolutionary Microbiology*, 54 (6), 2275-2279.

Facchini, M. C., Rinaldi, M., Decesari, S., Carbone, C., Finessi, E., Mircea, M., Fuzzi, S., Ceburnis, D., Flanagan, R., Nilsson, E. D., & Leeuw, G. 2008. Primary submicron marine aerosol dominated by insoluble organic colloids and aggregates. *Geophysical Research Letters*, 35 (17), L17814, doi:10.1029/2008GL034210

Fan, J., Leung, L. R., Rosenfeld, D., & DeMott, P. J. 2017. Effects of cloud condensation nuclei and ice nucleating particles on precipitation processes and supercooled liquid in mixed-phase orographic clouds. *Atmospheric Chemistry and Physics*, 17 (2), 1017-1035.

Fletcher, N. H. 1959. On ice-crystal production by aerosol particles. *Journal of Meteorology*, 16 (2), 173-180.

Freedman, M. A, 2015. Potential sites for ice nucleation on aluminosilicate clay minerals and related materials. *The Journal of Physical Chemistry Letters*, 6 (19), 3850-3858.

Fröhlich-Nowoisky, J., Nespoli, C. R., Pickersgrill, D. A., Galand, P. E., Müller-Germann, I., Nunes, T., Cardoso, J. G., Almeida, S. M., Pio, C., Andreae, M. O., & Conrad, R. 2014. Diversity and seasonal dynamics of airborne archaea. *Biogeosciences,* 11 (21), 6067-6079.

Fröhlich-Nowoisky, J., Kampf, C. J., Weber, B., Huffman, J. A., Pöhlker, C., Andreae, M. O., Lang-Yona, N., Burrows, S. M., Gunthe, S. S., Elbert, W., & Su, H. 2016. Bioaerosols in the Earth system: Climate, health, and ecosystem interactions. *Atmospheric Research*, 182, 346-378.

Gershey, R.M. 1983. Characterization of seawater organic matter carried by bubble-generated aerosols *Limnology and Oceanography*, 28, 309-319.

Gerten, D. & Adrian, R., 2000. Climate-driven changes in spring plankton dynamics and the sensitivity of shallow polymictic lakes to the North Atlantic Oscillation. *Limnology and Oceanography*, 45 (5), 1058-1066.

Gibbs, A., Charman, M., Schwarzacher, W., & Rust, A. C. 2015. Immersion freezing of supercooled water drops containing glassy volcanic ash particles. *GeoResJ*, *7*, 66-69.

Gibson, O. R., Taylor, L., Watt, P. W., & Maxwell, N. S. 2017. Cross-adaptation: heat and cold adaptation to improve physiological and cellular responses to hypoxia. *Sports Medicine*, 47 (9), 1751-1768.

Ginoux, P., Chin, M., Tegen, I., Prospero, J. M., Holben, B., Dubovik, O., & Lin, S. J. 2001. Sources and distributions of dust aerosols simulated with the GOCART model. *Journal of Geophysical Research: Atmospheres*, 106 (D17), 20255-20273.

Ginoux, P., Prospero, J. M., Torres, O., & Chin, M. 2004. Long-term simulation of global dust distribution with the GOCART model: correlation with North Atlantic Oscillation. *Environmental Modelling and Software*, 19 (2),113-128.

Gong, D. & Pickart, R. S. 2015. Summertime circulation in the eastern Chukchi Sea. *Topical Studies in Oceanography*, 118, 18-31.

Graf, H. F. 2004. The complex interaction of aerosols and clouds. *Science*, 303 (5662), 1309-1311.

Graversen, R. G. & Wang, M. 2009. Polar amplification in a coupled climate model with locked albedo. *Climate Dynamics*, 33 (5), 629-643.

Grebmeier, J. M. 2012. Shifting patterns of life in the Pacific Arctic and sub-Arctic seas. *Annual Review of Marine Science*, 4, 63-78.

Grebmeier, J. M., Moore, S. E., Cooper, L. W., Frey, K. E., & Pickart, R. S. 2012. The Distributed Biological Observatory (DBO): A change detection array in the Pacific Arctic region. *American Geophysical Union 2012 Fall Meeting Abstracts*, OS54A-02.

Grenfell, T. C. & Perovich, D. K. 1984. Spectral albedos of sea ice and incident solar irradiance in the southern Beaufort Sea. *Journal of Geophysical Research: Oceans*, 89 (C3), 3573-3580.

Guo, J., Liu, H., Li, Z., Rosenfeld, D., Jiang, M., Xu, W., Jiang, J. H., He, J., Chen, D., Min, M., & Zhai, P. 2018. Aerosol-induced changes in the vertical structure of precipitation: a perspective of TRMM precipitation radar. *Atmospheric Chemistry and Physics*, 18 (18), 13329-13343.

Hader, J. D., Wright, T. P. & Petters, M. D. 2014. Contribution of pollen to atmospheric ice nuclei concentrations. *Atmospheric Chemistry and Physics*, 14 (11), 5433-5449.

Hallegraeff, G.M., 2016. Seafood quality assurance for algal toxins. In: Daczkowska-Kozon, E.G. & Sun Pan, B. (Eds.), *Environmental Effects on Seafood Availability, Safety, and Quality*, CRC Press: Boca Raton, pp. 201-224.

Hande, L. B., Hoose, C., & Barthlott, C. 2017. Aerosol-and droplet-dependent contact freezing: Parameterization development and case study. *Journal of the Atmospheric Sciences*, 74 (7), 2229-2245.

Harrison, R. M. & Pio, C. A. 1983. Size-differentiated composition of inorganic atmospheric aerosols of both marine and polluted continental origin. *Atmospheric Environment*, 17 (9), 1733-1738.

Hartmann, S., Augustin, S., Clauss, T., Voigtländer, J., Niedermeier, D., Wex, H., & Stratmann, F. 2013. Immersion freezing of ice nucleating active protein complexes. *Atmospheric Chemistry and Physics*, 13, 5751-5766.

Haywood, J. 2016. Atmospheric aerosols and their role in climate change. In: Letcher, T.M. (Ed.), *Climate Change: Observed Impacts on Planet Earth*, Elsevier: Amsterdam, pp. 449-463.

Herbert, R. J., Murray, B. J., Dobbie, S. J., & Koop, T. 2015. Sensitivity of liquid clouds to homogenous freezing parameterizations. *Geophysical Research Letters*, 42 (5), 1599-1605.

Hill, T. C., DeMott, P. J., Tobo, Y., Fröhlich-Nowoisky, J., Moffett, B.F., Franc, G. D., & Kreidenweis, S. M. 2016. Sources of organic ice nucleating particles in soils. *Atmospheric Chemistry and Physics*, 16 (11), 7195-7211.

Hill, V. and Cota, G. 2005. Spatial patterns of primary production on the shelf, slope and basin of the Western Arctic in 2002. *Deep Sea Research Part II: Topical Studies in Oceanography*, 52 (24-26), 3344-3354.

Hiranuma, N., Paukert, M., Steinke, I., Zhang, K., Kulkarni, G., Hoose, C., Schnaiter, M., Saathoff, H., & Möhler, O. 2014. A comprehensive parameterization of heterogeneous ice nucleation of dust surrogate: laboratory study with hematite particles and its application to atmospheric models. *Atmospheric Chemistry and Physics*, 14 (23), 13145-13158.

Hoagland, K. D., Rosowski, J. R., Gretz, M. R., & Roemer, S. C. 1993. Diatom extracellular polymeric substances: function, fine structure, chemistry, and physiology. *Journal of Phycology*, 29 (5), 537-566.

Hu, C., Lee, Z. & Franz, B. 2012. Chlorophyll algorithms for oligotrophic oceans: A novel approach based on three-band reflectance difference. *Journal of Geophysical Research: Oceans*, 117 (C1), C01011, doi:10.1029/2011JC007395 .

Huang, W. T. K., Ickes, L., Tegen, I., Rinaldi, M., Ceburnis, D., & Lohmann, U. 2018. Global relevance of marine organic aerosol as ice nucleating particles. *Atmospheric Chemistry and Physics*, 18 (15), 11423-11445.

Hubanks, P. A., King, M. D., Platnick, S., & Pincus, R. 2008. MODIS atmosphere L3 gridded product algorithm theoretical basis document. *Algorithm Theoretical Baseline Document Reference Number: ATBD-MOD-30*, 30, 96.

Huffman, J. A., Prenni, A. J., DeMott, P. J., Pöhlker, C., Mason, R. H., Robinson, N. H., Fröhlich-Nowoisky, J., Tobo, Y., Després, V. R., Garcia, E., & Gochis, D. J. 2013. High concentrations of biological aerosol particles and ice nuclei during and after rain. *Atmospheric Chemistry and Physics*, 13 (13), 6151-6164.

Iken, K., Mueter, F., Grebmeier, J. M., Cooper, L. W., Danielson, S. L., & Bluhm, B. A. In press. Developing an observational design for epibenthos and fish assemblages in the Chukchi Sea. *Topical Studies in Oceanography*, doi:10.1016/j.dsr2.2018.11.005

Irving, L. 2012. Arctic life of birds and mammals: including man (Vol. 2). Springer Science & Business Media.

Jeffries, M. O., Richter-Menge, J., & Overland, J. E. 2015. Arctic report card. *NOAA, Pacific Marine Environmental Laboratory, Seattle, WA*, www.arctic.noaa.gov/Report-Card.

Johannessen, O. M., Kuzmina, S. I., Bobylev, L. P., & Miles, M. W. 2016. Surface air temperature variability and trends in the Arctic: new amplification assessment and regionalization. *Tellus A: Dynamic Meteorology and Oceanography*, 68 (1), 28234.

Kanji, Z. A. & Abbatt, J. P, 2006. Laboratory studies of ice formation via deposition mode nucleation onto mineral dust and n-hexane soot samples. *Journal of Geophysical Research: Atmospheres*, 111 (D16), D16204, doi:10.1029/2005JD006766

Kanji, Z. A., Ladino, L. A., Wex, H., Boose, Y., Burkert-Kohn, M., Cziczo, D. J., & Krämer, M. 2017. Overview of ice nucleating particles. *Meteorological Monographs*, 58, 1-1 – 1-33.

Kärcher, B., Mayer, B., Gierens, K., Burkhardt, U., Mannstein, H., & Chatterjee, R. 2009. Aerodynamic contrails: Microphysics and optical properties. *Journal of the Atmospheric Sciences*, 66 (2), 227-243.

Karner, M. B., DeLong, E. F., & Karl, D. M. 2001. Archaeal dominance in the mesopelagic zone of the Pacific Ocean, *Nature*, 409 (6819), 507-510.

Kauko, H. M., Pavlov, A. K., Johnsen, G., Granskog, M. A., Peeken, I., & Assmy, P. 2019. Photoacclimation state of an Arctic under-ice phytoplankton bloom. *Journal of Geophysical Research: Oceans*, 124(3), 1750-1762.

Khain, A. P., Rosenfeld, D., & Pokrovsky, A. 2001. Simulating convective clouds with sustained supercooled liquid water down to −37.5 C using a spectral microphysics model. *Geophysical Research Letters*, 28 (20), 3887-3890.

Kirkby, J., and 77 others. 2016. Ion-induced nucleation of pure biogenic particles. *Nature*, 533 (7604), 521-526.

Kulmala, M. 2003. How particles nucleate and grow. *Science*, 302 (5647), 1000-1001.

Kunkel, B. A. 1984. Parameterization of droplet terminal velocity and extinction coefficient in fog models. *Journal of Climate and Applied Meteorology*, 23 (1), 34-41.

Lacis, A. A. & Hansen, J. 1974. A parameterization for the absorption of solar radiation in the earth's atmosphere. *Journal of the Atmospheric Sciences*, 31 (1),118-133.

Laidre, K. L., Stern, H., Kovacs, K. M., Lowry, L., Moore, S. E., Regehr, E. V., Ferguson, S. H., Wiig, Ø., Boveng, P., Angliss, R. P., & Born, E. W. 2015. Arctic marine mammal population status, sea ice habitat loss, and conservation recommendations for the 21st century. *Conservation Biology*, 29 (3), 724-737.

Lammers, R. B., Shiklomanov, A. I., Vörösmarty, C. J., Fekete, B. M., & Peterson, B. J. 2001. Assessment of contemporary Arctic river runoff based on observational discharge records. *Journal of Geophysical Research: Atmospheres*, 106 (D4), 3321-3334.

Lana, A., Simó, R., Vallina, S. M., & Dachs, J. 2012. Potential for a biogenic influence on cloud microphysics over the ocean: a correlation study with satellite-derived data. *Atmospheric Chemistry and Physics*, 12 (17), 7977-7993.

Lange, R., Dall'Osto, M., Skov, H., Nøjgaard, J. K., Nielsen, I. E., Beddows, D. C. S., Simó, R., Harrison, R. M., & Massling, A. 2018. Characterization of distinct Arctic aerosol accumulation modes and their sources. *Atmospheric Environment*, 183, 1-10.

Langham, E. J. & Mason, B. J. 1958. The heterogeneous and homogeneous nucleation of supercooled water. *Proceedings of the Royal Society of London Series A: Mathematical and Physical Sciences*, 247, 493–504.

Leck, C. & Bigg, E. K. 2005. Source and evolution of the marine aerosol—A new perspective. *Geophysical Research Letters*, 32 (19), L19803, doi:10.1029/2005GL023651

Lindsay, M. R., Anderson, C., Fox, N., Scofield, G., Allen, J., Anderson, E., Bueter, L., Poudel, S., Sutherland, K., Munson-McGee, J. H., & Van Nostrand, J. D. 2017. Microbialite response to an anthropogenic salinity gradient in Great Salt Lake, Utah. *Geobiology,* 15 (1), 131-145.

Mason, R. H., Si, M., Li, J., Chou, C., Dickie, R., Toom-Sauntry, D., Pöhlker, C., Yakobi-Hancock, J. D., Ladino, L. A., Jones, K., & Leaitch, W. R. 2015. Ice nucleating particles at a coastal marine boundary layer site: correlations with aerosol type and meteorological conditions. *Atmospheric Chemistry and Physics*, 15 (21), 12547-12566.

Massana, R., Murray, E., Preston, C. M., & DeLong, E. F. 1997. Vertical distribution and phylogenetic characterization of marine planktonic Archaea in the Santa Barbara channel. *Applied and Environmental Microbiology*, 63, 50-56.

McCluskey, C. S., Ovadnevaite, J., Rinaldi, M., Atkinson, J., Belosi, F., Ceburnis, D., Marullo, S., Hill, T. C., Lohmann, U., Kanji, Z. A., & O'Dowd, C. 2018. Marine and terrestrial organic ice nucleating particles in pristine marine to continentally-influenced northeast Atlantic air masses. *Journal of Geophysical Research: Atmospheres*, 123 (11), 6196-6212.

McCoy, D. T., Burrows, S. M., Wood, R., Grosvenor, D. P., Elliott, S. M., Ma, P. L., Rasch, P. J., & Hartmann, D. L. 2015. Natural aerosols explain seasonal and spatial patterns of Southern Ocean cloud albedo. *Science Advances*, 1 (6), 150-157.

Meiners, K. M. & Michel, C. 2017. Dynamics of nutrients dissolved organic matter and exopolymers in sea ice. In: Thomas, D.N. (Ed.) *Sea Ice* (3rd ed.), Wiley: Chichester, pp. 415-432.

Meskhidze, N. & Nenes, A. 2006. Phytoplankton and cloudiness in the Southern Ocean. *Science*, 314 (5804), 1419-1423.

Meyers, M. P., DeMott, P. J., & Cotton, W. R. 1992. New primary ice-nucleation parameterizations in an explicit cloud model. *Journal of Applied Meteorology*, 31 (7), 708-721.

Monks, S. A., Arnold, S. R., Emmons, L. K., Law, K. S., Turquety, S., Duncan, B. N., Flemming, J., Huijnen, V., Tilmes, S., Langner, J., & Mao, J. 2015. Multi-model study of chemical and physical controls on transport of anthropogenic and biomass burning pollution to the Arctic. *Atmospheric Chemistry and Physics*, 15 (6), 3575-3603.

Moore, T. S., Campbell, J. W. & Dowell, M. D. 2009. A class-based approach to characterizing and mapping the uncertainty of the MODIS ocean chlorophyll product. *Remote Sensing of Environment*, 113 (11), 2424-2430.

Mossop, S. C. 1976. Production of secondary ice particles during the growth of graupel by riming. *Quarterly Journal of the Royal Meteorological Society*, 102 (431), 45-57.

Murphy, N. D. 2003. Dehydration in cold clouds is enhanced by a transition from cubic to hexagonal ice. *Geophysical Research Letters*, 30 (23), 2230, doi:10.1029/2003GL018566

Mysak, L. A. & Venegas, S. A. 1998. Decadal climate oscillations in the Arctic: A new feedback loop for atmosphere-ice-ocean interactions. *Geophysical Research Letters*, 25 (19), 3607-3610.

Najafi, M. R., Zwiers, F. W., & Gillett, N. P. 2015. Attribution of Arctic temperature change to greenhouse-gas and aerosol influences. *Nature Climate Change*, *5* (3), 246-249.

Nakata, M. 2018. Analysis of climate change caused by aerosol-cloud-radiation interaction. *Proceedings of the SPIE*, 10786, 1078614, https://doi.org/10.1117/12.2325265

Nishino, S., Kikuchi, T., Fujiwara, A., Hirawake, T., & Aoyama, M. 2016. Water mass characteristics and their temporal changes in a biological hotspot in the southern Chukchi Sea. *Biogeosciences*, 13 (8), 2563-2578.

Nyman, E. 2018. Protecting the poles: Marine living resource conservation approaches in the Arctic and Antarctic. *Ocean and Coastal Management*, 151, 193-200.

O'Dowd, C. D. & De Leeuw, G. 2007. Marine aerosol production: a review of the current knowledge. *Philosophical Transactions of the Royal Society A: Mathematical, Physical and Engineering Sciences*, 365 (1856), 1753-1774.

O'Sullivan, D., Murray, B. J., Malkin, T. L., Whale, T. F., Umo, N. S., Atkinson, J. D., Price, H. C., Baustian, K. J., & Webb, M. E. 2014. Ice nucleation by fertile soil dusts: relative importance of mineral and biogenic components. *Atmospheric Chemistry and Physics*, 14 (4), 1853-1867.

O'Sullivan, D., Adams, M. P., Tarn, M. D., Harrison, A. D., Vergara-Temprado, J., Porter, G. C. E., Holden, M. A., Sanchez-Marroquin, A., Carotenuto, F., Whale, T. F., & McQuaid, J. B. 2018. Contributions of biogenic material to the atmospheric ice-nucleating particle population in north western Europe. *Scientific Reports*, 8 (1), 13821.

Oren, A. 2002. Molecular ecology of extremely halophilic archaea and bacteria. *FEMS Microbiology Ecology* 39 (1), 1-7.

Oren, A. 2008. Microbial life at high salt concentrations: phylogenetic and metabolic diversity. *Saline Systems*, 4 (1), 2.

Overland, J. E. & Roach, A. T. 1987. Northward flow in the Bering and Chukchi Seas. *Journal of Geophysical Research: Oceans*, 92 (C7), 7097-7105.

Palo, T., Vihma, T., Jaagus, J., & Jakobson, E. 2017. Observations of temperature inversions over central Arctic sea ice in summer. *Quarterly Journal of the Royal Meteorological Society*, 143 (708), 2741-2754.

Peralta-Ferriz, C. & Woodgate, R. A. 2015. Seasonal and interannual variability of pan-Arctic surface mixed layer properties from 1979 to 2012 from hydrographic data, and the dominance of stratification for multiyear mixed layer depth shoaling. *Progress in Oceanography*, 134, 19-53.

Perovich, D. K., Richter-Menge, J. A., Jones, K. F., & Light, B. 2008. Sunlight, water, and ice: Extreme Arctic sea ice melt during the summer of 2007. *Geophysical Research Letters*, 35 (11), L11501, doi:10.1029/2008GL034007

Pithan, F. & Mauritsen, T. 2014. Arctic amplification dominated by temperature feedbacks in contemporary climate models. *Nature Geoscience*, 7 (3), 181-184.

Poli, A., Di Donato, P., Abbamondi, G. R., & Nicolaus, B. 2011. Synthesis, production, and biotechnological applications of exopolysaccharides and polyhydroxyalkanoates by archaea. *Archaea*, 2011, 693253.

Pöschl, U. 2005. Atmospheric aerosols: composition, transformation, climate and health effects. *Angewandte Chemie International Edition*, 44 (46), 7520-7540.

Post, E., Bhatt, U. S., Bitz, C. M., Brodie, J. F., Fulton, T. L., Hebblewhite, M., Kerby, J., Kutz, S. J., Stirling, I., & Walker, D. A. 2013. Ecological consequences of sea-ice decline. *Science*, 341 (6145), 519-524.

Prathumratana, L., Sthiannopkao, S., & Kim, K. W. 2008. The relationship of climatic and hydrological parameters to surface water quality in the lower Mekong River. *Environment International*, 34 (6), 860-866.

Prenni, A. J., DeMott, P. J., Sullivan, A. P., Sullivan, R. C., Kreidenweis, S. M., & Rogers, D. C. 2012. Biomass burning as a potential source for atmospheric ice nuclei: Western wildfires and prescribed burns. *Geophysical Research Letters*, 39 (11), L11805, doi:10.1029/2012GL051915.

Pummer, B. G., Bauer, H., Bernardi, J., Bleicher, S., & Grothe, H. 2012. Suspendable macromolecules are responsible for ice nucleation activity of birch and conifer pollen, *Atmospheric Chemistry and Physics*, 12, 2541-2550,

Pummer, B. G., Budke, C., Augustin-Bauditz, S., Niedermeier, D., Felgitsch, L., Kampf, C. J., Huber, R. G., Liedl, K. R., Loerting, T., Moschen, T., & Schauperl, M. 2015. Ice nucleation by water-soluble macromolecules. *Atmospheric Chemistry and Physics*, 15 (8), 4077-4091.

Quinn, P. K., Shaw, G., Andrews, E., Dutton, E. G., Ruoho-Airola, T., & Gong, S. L. 2007. Arctic haze: current trends and knowledge gaps. *Tellus B: Chemical and Physical Meteorology*, 59 (1), 99-114

Quinn, P. K., Collins, D. B., Grassian, V. H., Prather, K. A., & Bates, T. S. 2015. Chemistry and related properties of freshly emitted sea spray aerosol. *Chemical Reviews*, 115 (10), 4383-4399.

Quinn, P. K., Coffman, D. J., Johnson, J. E., Upchurch, L. M., & Bates, T. S. 2017. Small fraction of marine cloud condensation nuclei made up of sea spray aerosol. *Nature Geoscience*, 10 (9), 674-679.

Ramanathan, V., Barkstom, B. R., & Harrison, E. F. 1989. Climate and the Earth's radiation budget. *Physics Today*, 42(5), 22-32.

Reddy, S. K., Thiraux, R., Rudd, B. A. W., Lin, L., Adel, T., Joutsuka, T., Geiger, F. M., Allen, H. C., Morita, A., & Paesani, F. 2018. Bulk contributions modulate the sum-frequency generation spectra of water on model sea-spray aerosols. *Chemistry*, 4 (7), 1629-1644.

Resch, F. J., Darrozes, J. S., & Afeti, G. M. 1986. Marine liquid aerosol production from bursting of air bubbles. *Journal of Geophysical Research: Oceans*, 91 (C1), 1019-1029.

Reynolds, R. L., Yount, J. C., Reheis, M., Goldstein, H., Chavez, P., Fulton, R., Whitney, J., Fuller, C., & Forester, R. M. 2007. Dust emission from wet and dry playas in the Mojave Desert, USA. *Earth Surface Processes and Landforms*, 32 (12), 1811-1827.

Richter, D. & Gill, T. E. 2018. Challenges and opportunities in atmospheric dust emission chemistry and transport. *Bulletin of the American Meteorological Society*, 99 (7), ES115-ES118.

Rothschild, L. J. & Mancinelli, R. L. 2001. Life in extreme environments. *Nature*, 409 (6823), 1092-1101.

Rudels, B., Jones, E. P., Anderson, L. G., & Kattner, G. 1994. On the intermediate depth waters of the Arctic Ocean. In: Johannessen, O.M., Muench, R.D., & Overland, J.E. (Eds.) The Polar Oceans and Their Role in Shaping the Global Environment. *Geophysical Monograph Series*, 85, 33-46.

Šantl-Temkiv, T., Sahyoun, M., Finster, K., Hartmann, S., Augustin-Bauditz, S., Stratmann, F., Wex, H., Clauss, T., Nielsen, N. W., Sørensen, J. H., & Korsholm, U. S. 2015. Characterization of airborne ice-nucleation-active bacteria and bacterial fragments. *Atmospheric Environment*, 109, 105-117.

Schleifer, K. H., Steber, J., & Mayer, H. 1982. Chemical composition and structure of the cell wall of Halococcus morrhuae. *Zentralblatt für Bakteriologie Mikrobiologie und Hygiene: Originale: Allgemeine, Angewandte und Okologische Mikrobiologie*, 3 (2), 171-178.

Schleper, C., Jurgens, G., & Jonuscheit, M. 2005. Genomic studies of uncultivated archaea. *Nature Reviews Microbiology*, 3 (6), 479-488.

Screen, J. A. & Simmonds, I. 2010. The central role of diminishing sea ice in recent Arctic temperature amplification. *Nature*, 464 (7293), 1334-1337.

Seinfeld, J. H., Bretherton, C., Carslaw, K. S., Coe, H., DeMott, P. J., Dunlea, E. J., Feingold, G., Ghan, S., Guenther, A. B., Kahn, R., & Kraucunas, I. 2016. Improving our fundamental understanding of the role of aerosol−cloud interactions in the climate system. *Proceedings of the National Academy of Sciences (USA)*, 113 (21), 5781-5790.

Semeniuk, K. & Dastoor, A. 2018. Current state of aerosol nucleation parameterizations for air-quality and climate modeling. *Atmospheric Environment*, 179, 77-106.

Serreze, M. C. & Barry, R. G. 2011. Processes and impacts of Arctic amplification: A research synthesis. *Global and Planetary Change*, 77 (1-2), 85-96.

Serreze, M. C., Walsh, J. E., Chapin, F. S., Osterkamp, T., Dyurgerov, M., Romanovsky, V., Oechel, W. C., Morison, J., Zhang, T., & Barry, R. G. 2000. Observational evidence of recent change in the northern high-latitude environment. *Climatic Change*, 46 (1-2), 159-207.

Serreze, M. C., Crawford, A. D., Stroeve, J. C., Barrett, A. P., & Woodgate, R. A. 2016. Variability, trends, and predictability of seasonal sea ice retreat and advance in the Chukchi Sea. *Journal of Geophysical Research: Oceans*, 121 (10), 7308-7325.

Shupe, M., 2016. Final Report: Investigations of mixed-phase cloud microphysical, radiative, and dynamical processes. *USDOE Office of Science*, Web. doi:10.2172/1298132.

Shupe, M. D., Persson, P. O. G., Brooks, I. M., Tjernström, M., Sedlar, J., Mauritsen, T., Sjogren, S., & Leck, C. 2013. Cloud and boundary layer interactions over the Arctic sea ice in late summer. *Atmospheric Chemistry and Physics*, 13 (18), 9379-9399.

Sihvonen, S. K., Schill, G. P., Lyktey, N. A., Veghte, D. P., Tolbert, M. A., & Freedman, M. A. 2014. Chemical and physical transformations of aluminosilicate clay minerals due to acid treatment and consequences for heterogeneous ice nucleation. *The Journal of Physical Chemistry*, 118 (38), 8787-8796.

Simó, R. 2001. Production of atmospheric sulfur by oceanic plankton: biogeochemical, ecological and evolutionary links. *Trends in Ecology and Evolution*, 16 (6), 287-294.

Smith, D. M., Dunstone, N. J., Scaife, A. A., Fiedler, E. K., Copsey, D., & Hardiman, S. C. 2017. Atmospheric response to Arctic and Antarctic sea ice: The importance of ocean–atmosphere coupling and the background state. *Journal of Climate*, 30 (12), 4547-4565.

Stabeno, P., Kachel, N., Ladd, C., & Woodgate, R. 2018. Flow patterns in the eastern Chukchi Sea: 2010–2015. *Journal of Geophysical Research: Oceans*, 123 (2), 1177-1195.

Stein, R., Fahl, K., Schade, I., Manerung, A., Wassmuth, S., Niessen, F., & Nam, S. I. 2017. Holocene variability in sea ice cover, primary production, and Pacific-Water inflow and climate change in the Chukchi and East Siberian Seas (Arctic Ocean). *Journal of Quaternary Science*, 32 (3), 362-379.

Stopelli, E., Conen, F., Zimmermann, L., Alewell, C., & Morris, C. E. 2014. Freezing nucleation apparatus puts new slant on study of biological ice nucleators in precipitation, *Atmospheric Measurement Techniques*, 7, 129-134.

Storelvmo, T. 2017. Aerosol effects on climate via mixed-phase and ice clouds. *Annual Review of Earth and Planetary Sciences*, 45, 199-222.

Stroeve, J. C., Crawford, A. D., & Stammerjohn, S. 2016. Using timing of ice retreat to predict timing of fall freeze-up in the Arctic. *Geophysical Research Letters*, 43 (12), 6332-6340.

Sun, L., Perlwitz, J., & Hoerling, M. 2016. What caused the recent "warm Arctic, cold continents" trend pattern in winter temperatures? *Geophysical Research Letters*, *43* (10), 5345-5352.

Suresh-Kumar, A., Mody, K., & Jha, B. 2007. Bacterial exopolysaccharides–a perception. *Journal of Basic Microbiology*, 47 (2), 103-117.

Suzuki, K., Stephens, G. L., & Golaz, J. C. 2017. Significance of aerosol radiative effect in energy balance control on global precipitation change. *Atmospheric Science Letters*, 18 (10), 389-395.

Tao, W. K., Chen, J. P., Li, Z., Wang, C., & Zhang, C. 2012. Impact of aerosols on convective clouds and precipitation. *Reviews of Geophysics*, 50, RG2001, doi:10.1029/2011RG000369.

Tobo, Y. 2016. An improved approach for measuring immersion freezing in large droplets over a wide temperature range, *Scientific Reports*, 6, 32930.

Tobo, Y., Prenni, A. J., DeMott, P. J., Huffman, J. A., McCluskey, C. S., Tian, G., Pöhlker, C., Pöschl, U., & Kreidenweis, S. M. 2013. Biological aerosol particles as a key determinant of ice nuclei populations in a forest ecosystem. *Journal of Geophysical Research: Atmospheres*, 118 (17), 10100-10110.

Tobo, Y., Adachi, K., DeMott, P. J., Hill, T. C., Hamilton, D. S., Mahowald, N. M., Nagatsuka, N., Ohata, S., Uetake, J., Kondo, Y., & Koike, M. 2019. Glacially sourced dust as a potentially significant source of ice nucleating particles. *Nature Geoscience*, 12, 253-258.

Tomasi, C., Lanconelli, C., Mazzola, M., & Lupi, A. 2017. Aerosol and Climate Change: Direct and Indirect Aerosol Effects on Climate. In: Tomasi, C., Fuzzi, S., & Kokhanovsky, A. (Eds.) 2017. *Atmospheric aerosols: Life cycles and effects on air quality and climate*. Wiley: Chichester, pp. 437-451.

Tourney, J. & Ngwenya, B. T. 2014. The role of bacterial extracellular polymeric substances in geomicrobiology. *Chemical Geology*, 386, 115-132.

Tremblay, J. E., Michel, C., Hobson, K. A., Gosselin, M., & Price, N. M., 2006. Bloom dynamics in early opening waters of the Arctic Ocean. *Limnology and Oceanography*, 51 (2), 900-912.

Turner, D. D., Shupe, M. D., & Zwink, A. B. 2018. Characteristic atmospheric radiative heating rate profiles in Arctic clouds as observed at Barrow, Alaska. *Journal of Applied Meteorology and Climatology*, 57 (4), 953-968.

Vali, G. & Stansbury, E.J. 1966. Time-dependent characteristics of the heterogeneous nucleation of ice. *Canadian Journal of Physics*, 44(3), 477-502.

Vali, G., DeMott, P. J., Möhler, O., & Whale, T. F. 2015. Technical Note: A proposal for ice nucleation terminology. *Atmospheric Chemistry and Phys*ics, 15 (18), 10263-10270.

Van Der Does, M., Knippertz, P., Zschenderlein, P., Harrison, R. G., & Stuut, J. B. W. 2018. The mysterious long-range transport of giant mineral dust particles. *Science Advances*, 4 (12): eaau2768.

Ventosa, A. 2006. Unusual micro-organisms from unusual habitats: hypersaline environments. *Symposia-Society for Microbiology*, (66), 223-226.

Vergara-Temprado, J., Miltenberger, A. K., Furtado, K., Grosvenor, D. P., Shipway, B. J., Hill, A.A., Wilkinson, J.M., Field, P.R., Murray, B.J., & Carslaw, K.S. 2018. Strong control of Southern Ocean cloud reflectivity by ice-nucleating particles. *Proceedings of the National Academy of Sciences (USA)*, 115 (11), 2687-2692.

Veron, F. 2015. Ocean spray. *Annual Review of Fluid Mechanics*, *47*, 507-538.

Vinogradova, A. 2015. Anthropogenic black carbon emissions to the atmosphere: surface distribution through Russian territory. *Atmospheric and Oceanic Optics*, 28 (2), 158-164.

Wadhams, P. 2000. *Ice in the ocean*. London: CRC Press.

Wagner, R., Kiselev, A., Moehler, O., Saathoff, H. & Steinke, I. 2016. Pre-activation of ice-nucleating particles by the pore condensation and freezing mechanism. *Atmospheric Chemistry and Physics*, 16 (4), 2025-2042.

Wall, S. M., John, W., & Ondo, J. L. 1988. Measurement of aerosol size distributions for nitrate and major ionic species. *Atmospheric Environment*, 22 (8), 1649-1656.

Wallace, J.M. & Hobbs, P.V. 2006. *Atmospheric science: an introductory survey*. Academic Press.

Walsh, J. E. 2008. Climate of the Arctic marine environment. *Ecological Applications*, 18 (SP2), S3-S22.

Walsh, J. E., Bromwich, D. H., Overland, J. E., Serreze, M. C., & Wood, K. R., 2018. 100 years of progress in polar meteorology. *Meteorological Monographs*, 59, 21-1 – 21-36.

Wan, Z., Zhang, Y., Zhang, Q. & Li, Z. L. 2002. Validation of the land-surface temperature products retrieved from Terra moderate resolution imaging spectroradiometer data. *Remote Sensing of Environment*, 83 (1-2), 163-180.

Wang, Q., Wekerle, C., Danilov, S., Koldunov, N., Sidorenko, D., Sein, D., Rabe, B., & Jung, T. 2018. Arctic sea ice decline significantly contributed to the unprecedented liquid freshwater accumulation in the Beaufort Gyre of the Arctic Ocean. *Geophysical Research Letters*, 45 (10), 4956-4964.

Wang, X., Deane, G. B., Moore, K. A., Ryder, O.S., Stokes, M. D., Beall, C. M., Collins, D. B., Santander, M. V., Burrows, S. M., Sultana, C. M., & Prather, K. A. 2017. The role of jet and film drops in controlling the mixing state of submicron sea spray aerosol particles. *Proceedings of the National Academy of Sciences (USA)*, 114 (27), 6978-6983.

Wehking, J., Pickersgill, D. A., Bowers, R. M., Teschner, D., Pöschl, U., Fröhlich-Nowoisky, J., & Després, V. R. 2018. Community composition and seasonal changes of archaea in coarse and fine air particulate matter. *Biogeosciences*, 15 (13), 4205-4214.

Weingartner, T., Aagaard, K., Woodgate, R., Danielson, S., Sasaki, Y., & Cavalieri, D. 2005. Circulation on the north central Chukchi Sea shelf. *Topical Studies in Oceanography*, 52 (24), 3150-3174.

Welti, A., Lüönd, F., Stetzer, O., & Lohmann, U. 2009. Influence of particle size on the ice nucleating ability of mineral dusts. *Atmospheric Chemistry and Physics*, 9 (18), 6705-6715.

Wex, H., Augustin-Bauditz, S., Boose, Y., Budke, C., Curtius, J., Diehl, K., Dreyer, A., Frank, F., Hartmann, S., Hiranuma, N., & Jantsch, E. 2015. Intercomparing different devices for the investigation of ice nucleating particles using Snomax® as test substance. *Atmospheric Chemistry and Physics*, *15* (3), 1463-1485.

Wilson, T. W., & 28 others. 2015. A marine biogenic source of atmospheric ice-nucleating particles. *Nature*, *525* (7568), 234-238.

Woese, C. R. & Fox, G. E. 1977. Phylogenetic structure of the prokaryotic domain: the primary kingdoms. *Proceedings of the National Academy of Sciences (USA),* 74 (11), 5088-5090.

Woese, C. R., Kandler, O., & Wheelis, M. L. 1990. Towards a natural system of organisms: proposal for the domains Archaea, Bacteria, and Eucarya. *Proceedings of the National Academy of Sciences (USA)*, 87 (12), 4576-4579.

Wright, T. P. & Petters, M. D. 2013. The role of time in heterogeneous freezing nucleation, *Journal of Geophysical Research: Atmospheres*, 118, 3731-3743.

Xie, Z., Sun, L., Blum, J. D., Huang, Y., & He, W., 2006. Summertime aerosol chemical components in the marine boundary layer of the Arctic Ocean. *Journal of Geophysical Research: Atmospheres*, *111* (D10), D10309, doi:10.1029/2005JD006253

Yarza, P., Yilmaz, P., Yarza, P., Yilmaz, P., Pruesse, E., Glöckner, F. O., Ludwig, W., Schleifer, K. H., Whitman, W. B., Euzéby, J., Amann, R., & Rosselló-Móra, R. 2014. Uniting the classification of cultured and uncultured bacteria and archaea using 16S rRNA gene sequences. *Nature Reviews Microbiology* 12 (9), 635-645.

Yun, M. S., Whitledge, T. E., Stockwell, D., Lee, J. H., Park, J. W., Lee, D. B., Park, J., & Lee, S. H. 2016. The potential effects of fresh water content on the primary production in the Chukchi Sea. *Biogeosciences*, 13, 737-749.

Zhang, S., Jiang, Y., Chen, C. S., Spurgin, J., Schwehr, K. A., Quigg, A., Chin, W. C., & Santschi, P. H. 2012. Aggregation, dissolution, and stability of quantum dots in marine environments: importance of extracellular polymeric substances. *Environmental Science and Technology*, 46 (16), 8764-8772.

Zhang, X., Alexander, L., Hegerl, G. C., Jones, P., Tank, A. K., Peterson, T. C., Trewin, B. & Zwiers, F. W., 2011. Indices for monitoring changes in extremes based on daily temperature and precipitation data. *Wiley Interdisciplinary Reviews: Climate Change*, 2 (6), 851-870.

Zhao, B., Liou, K. N., Gu, Y., Jiang, J. H., Li, Q., Fu, R., Huang, L., Liu, X., Shi, X., Su, H., & He, C. 2018. Impact of aerosols on ice crystal size. *Atmospheric Chemistry and Physics*, 18 (2), 1065-1078.

Zolles, T., Burkart, J., Häusler, T., Pummer, B., Hitzenberger, R., & Grothe, H. 2015. Identification of ice nucleation active sites on feldspar dust particles. *The Journal of Physical Chemistry*, 119 (11), 2692-2700.

Vita

Julio Eduardo Ceniceros is an environmental scientist with specialized training in geographic information systems and spatial analysis. His research experience includes remote sensing analysis of the ocean-air interface, lab analysis of microorganism ice nucleating abilities, and specialized field-work with meteorological and oceanic scientific equipment. He received his undergraduate degree in anthropology from the University of Texas at Austin in 2011 is now earning his Master's degree in environmental science from the University of Texas at El Paso in 2019. Julio has been accepted and plans on continuing with his higher education through earning a doctoral degree in environmental science and engineering also at the University of Texas at El Paso. He will observe, map, and analyze rapid coastal erosion in northern Alaska. Long-term goals include continued environmental research as part of a federal or academic lab specializing in remote sensing and field investigations.